Cosmic Ray Physics with ARGO-YBJ

Michele Iacovacci
University and INFN of Naples.
for the ARGO-YBJ collaboration

SCINEGHE 2012, Lecce

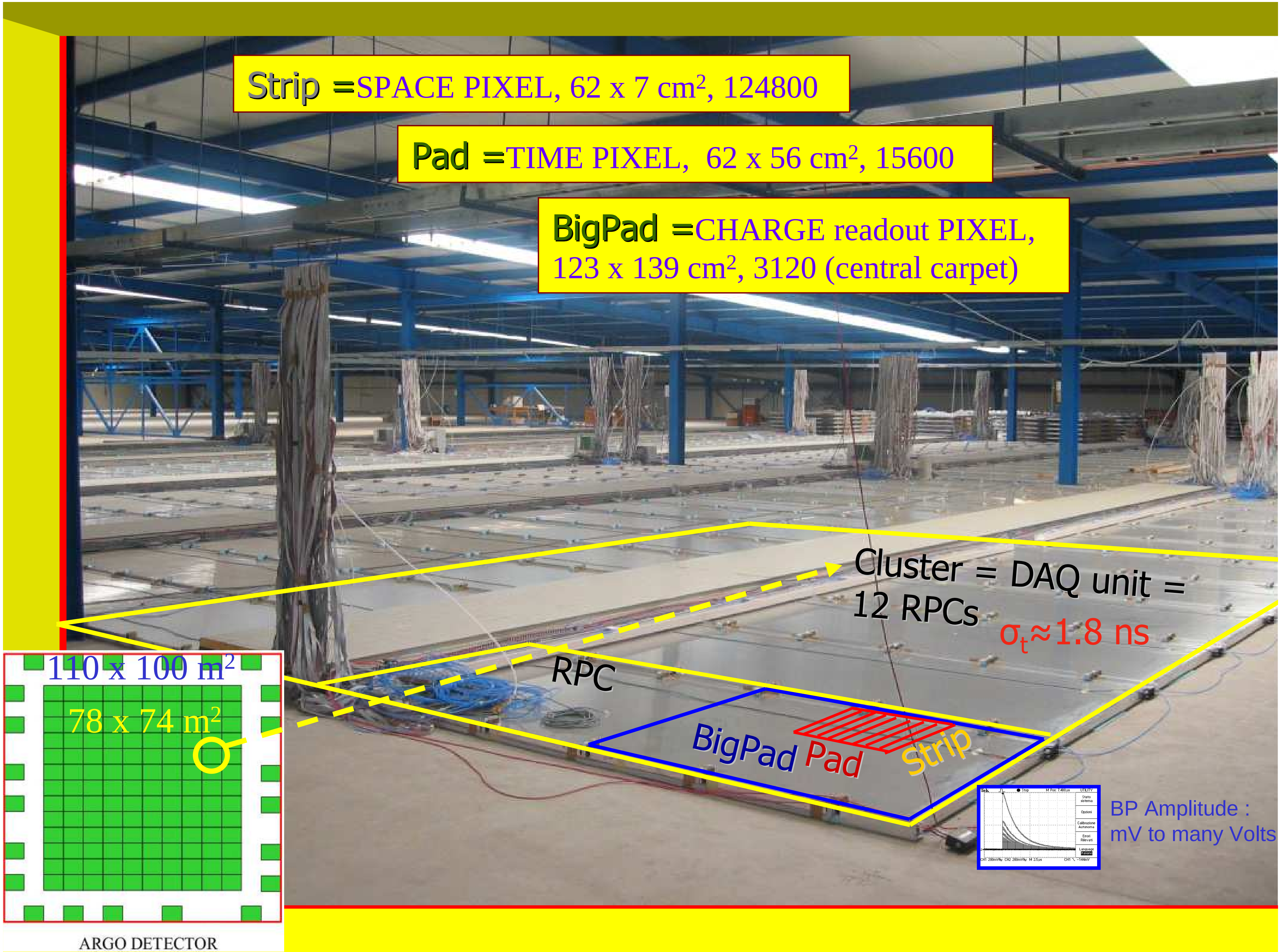
Strip =SPACE PIXEL, 62 x 7 cm², 124800
Pad =TIME PIXEL, 62 x 56 cm², 15600
BigPad =CHARGE readout PIXEL, 123 x 139 cm², 3120 (central carpet)
Cluster = DAQ unit = 12 RPCs
σt≈1.8 ns
RPC
BigPad
Pad
Strip
110 x 100 m²
78 x 74 m²
ARGO DETECTOR
BP Amplitude :
mV to many Volts

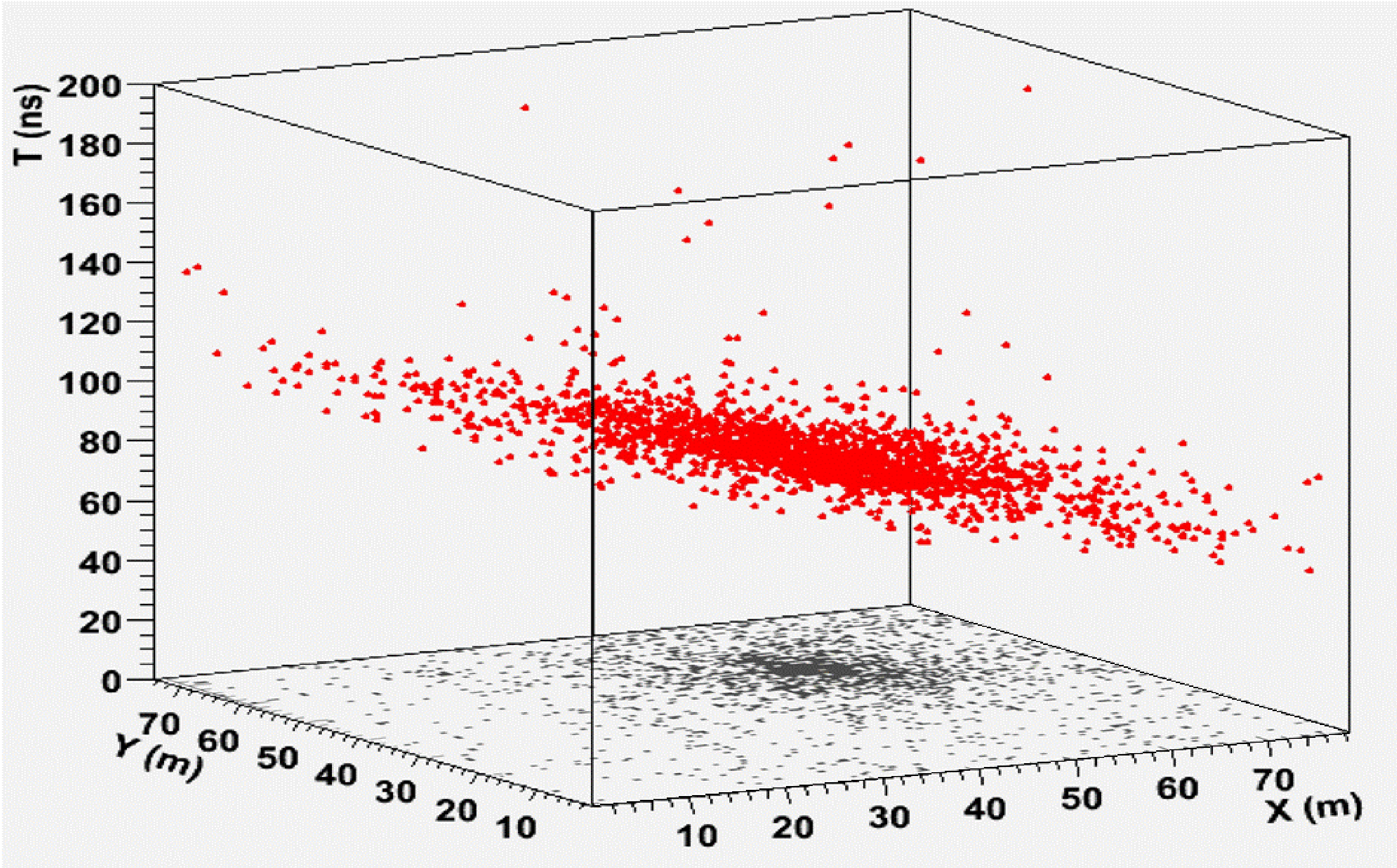

T (ns)
200
180
160
140
120
100
80
60
40
20
0
Y (m)
70
60
50
40
30
20
10
10
20
30
40
50
60
70
X (m)

Current status

- In operation since July 2006 (commissioning phase)
- Stable data taking since November 2007 with final configuration
- The average duty cycle ~ 85%
- Trigger rate ~3.5 kHz @ 20 pad threshold
- $\approx 4 \cdot 10^{11}$ events collected
- Dead time 4%
- 220 GB/day transferred to IHEP/CNAF data centres

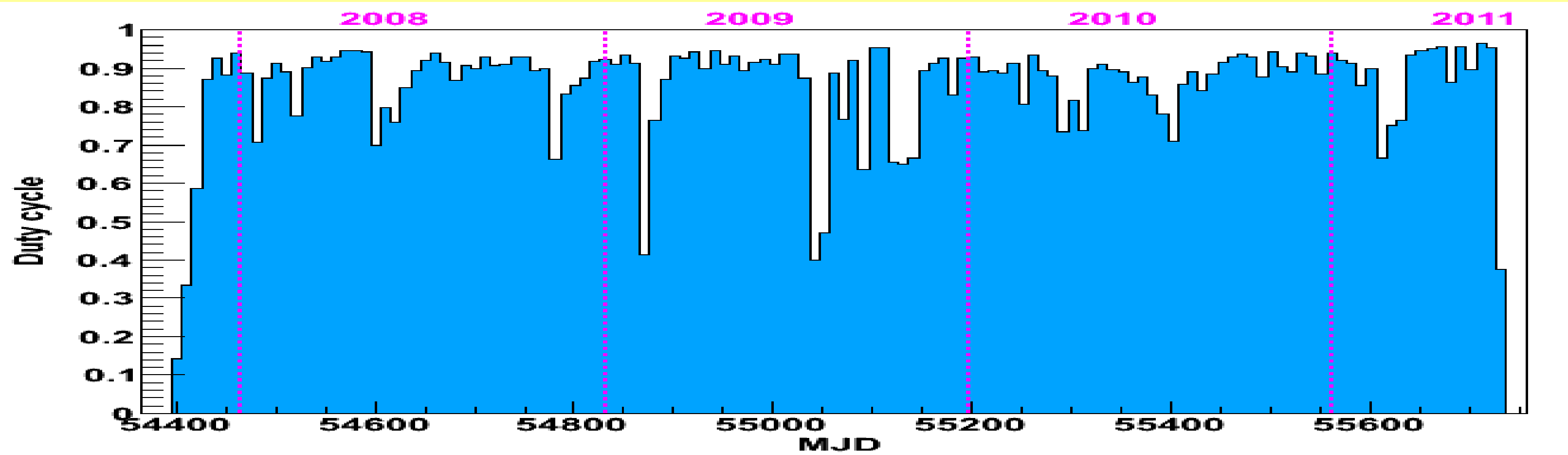

Moon shadow analysis

PRD 84 (2011) 022003

- A natural tool to evaluate the performance of the detector

The energy scale uncertainty is estimated to be smaller than 13% in the range 1 – 30 TeV/Z.

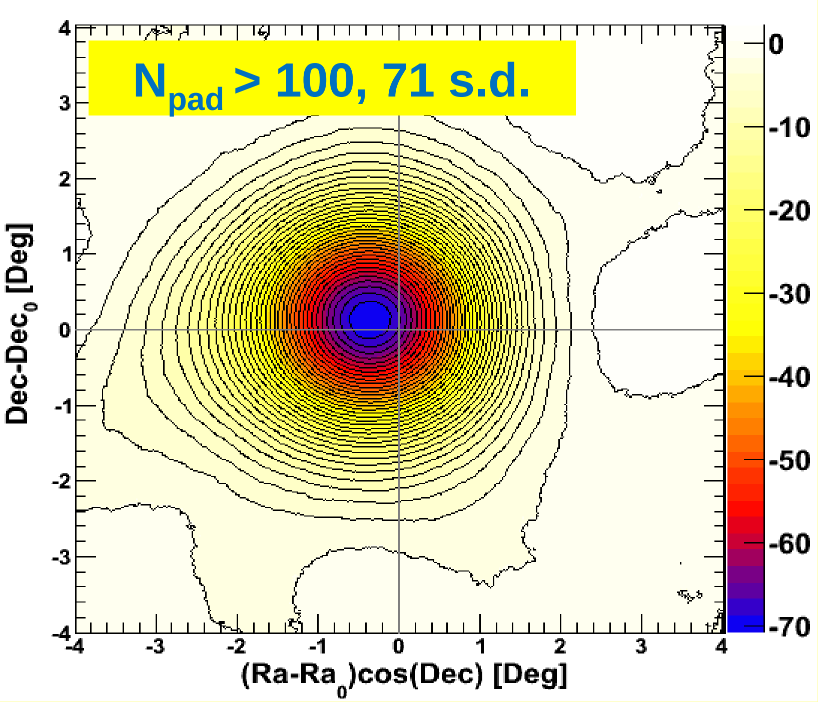

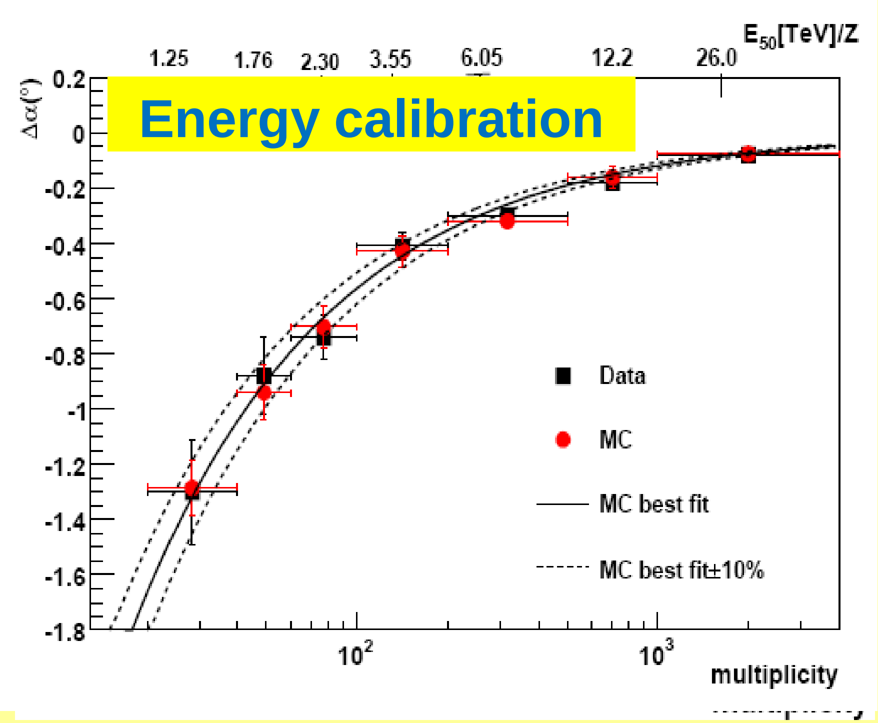

Upper limits on p̄/p by ARGO-YBJ

PRD 85 (2012) 022002

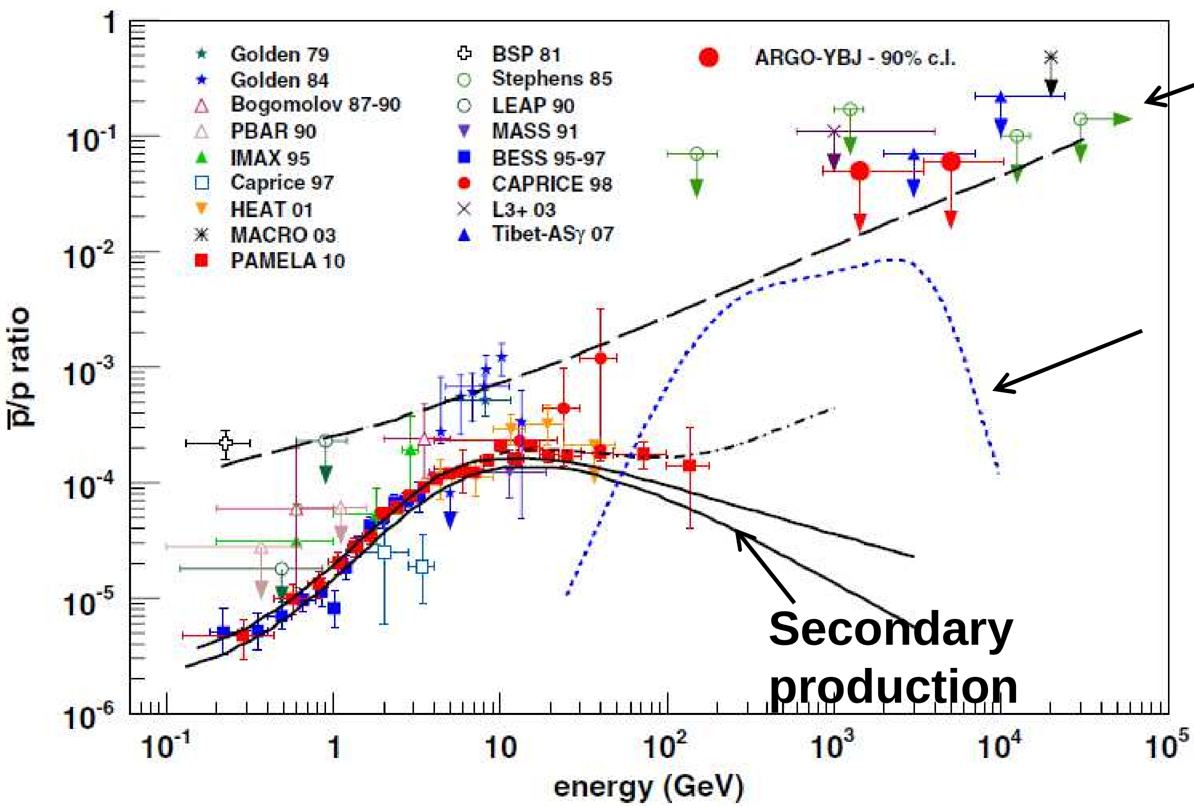

Antigalaxies contribution

Heavy DM contribution

In this energy range the p fraction in CR is ≈70%

5% at 1.4 TeV	at 90% c.l.
6% at 5 TeV	at 90% c.l.

Sun shadow

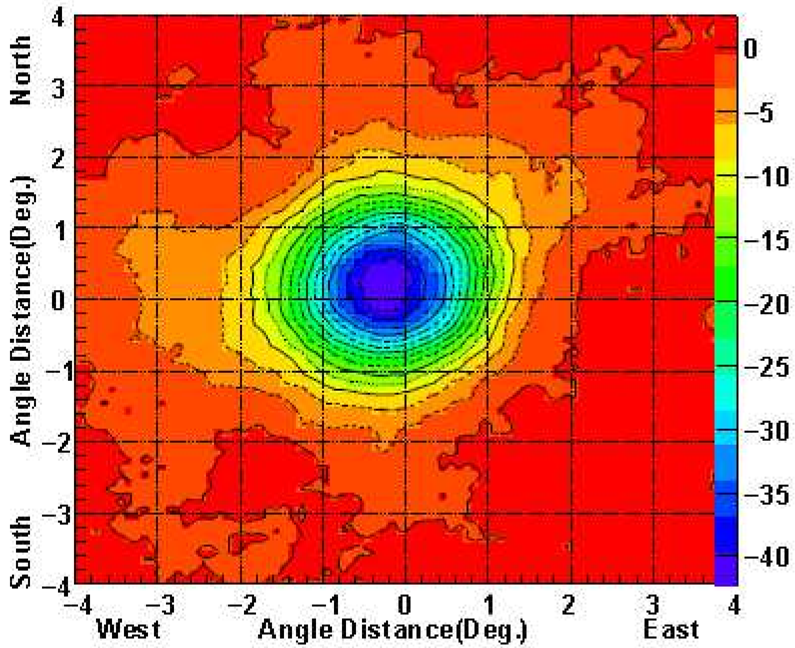

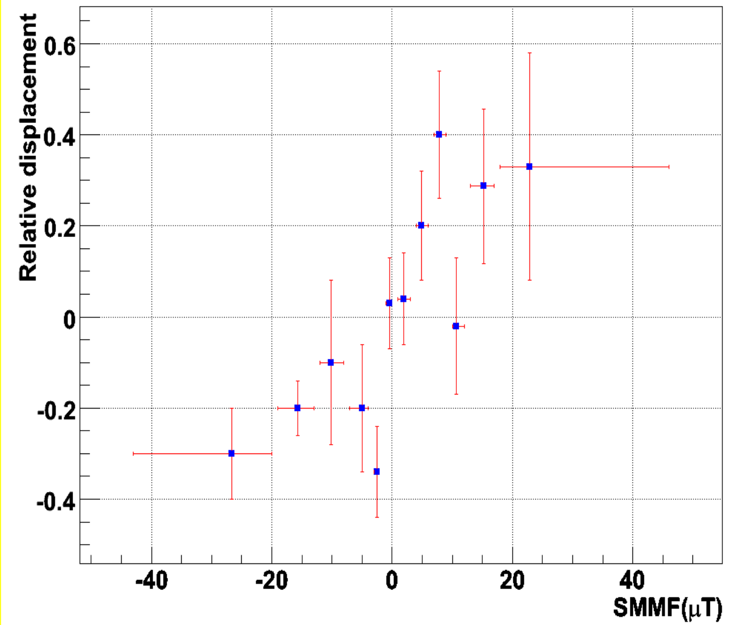

Displacement of the Sun shadow correlates with the SMMF

Sun at maximum → shadow is washed out
Sun at minimum → good shadow & SMF symmetric between NS

→ **EW shift due to GMF**
NS shift due to IMF

The displacement of the Sun shadow is a good measurement of the IMF, especially in a this particular quiet phase between 23th and 24th cycles.

Solar wind e IMF

radial velocity at emission v_r
+
run rotation

Archimedean spiral

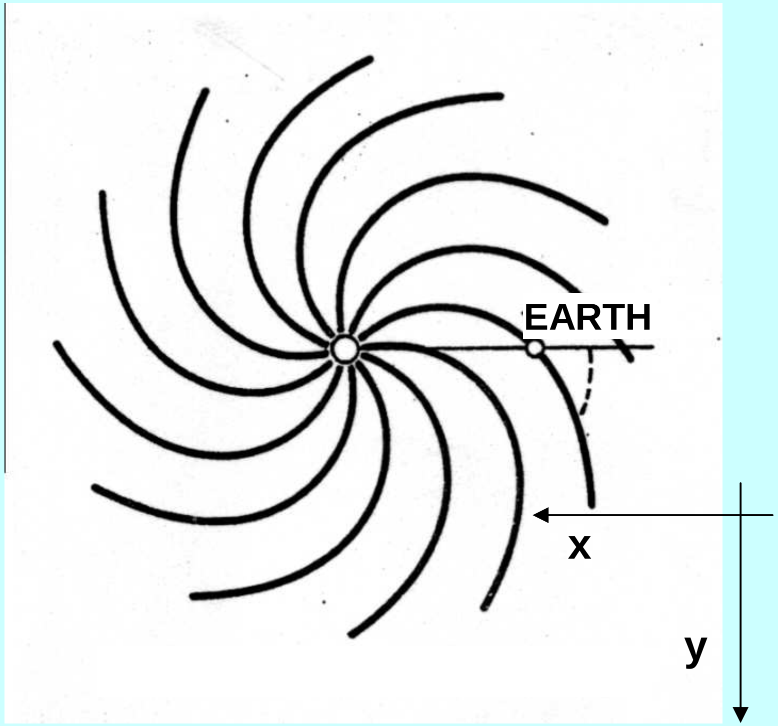

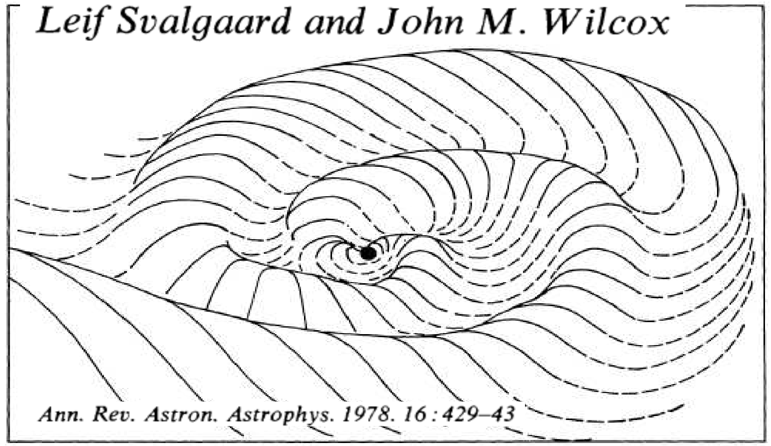

Figure 6 Sketch showing the warped current sheet in the inner solar system (inside of 6 au). This current sheet divides the interplanetary magnetic field in the heliosphere into two regions with oppositely directed field lines. In one region the field polarity is away from the Sun (at present this region is north of the solar equator), in the other region the field polarity is toward the Sun. The situation is shown for a four-sector structure and we try to depict the shape of a surface in three dimensions. Where this surface—in which the current flows—lies above the solar equatorial plane it is shown by full lines, while dashed lines indicate that the current sheet dips below the equatorial plane. The extent in latitude of the current sheet was assumed to be ±15°. The Sun at the center is not to scale (from Svalgaard & Wilcox 1976).

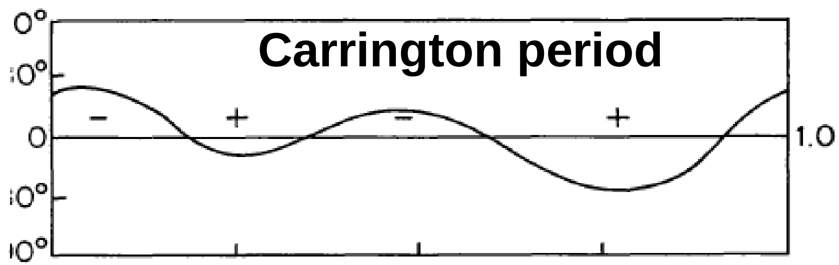

Computed neutral lines on a source surface at 2.6 solar radii

… so a charge particle that passes through the IMF experiences a B_y that changes once or twice from positive to negative (two or four sectors structure). Consenquently the sun shadow will be seen oscillating once or twice along north-south direction in a solar rotation period, or Carrington period.

IMF measurement with ARGO-YBJ

ApJ 729:113 (4pp), 2011

potential forecasting capability for magnetic storms due to solar events.

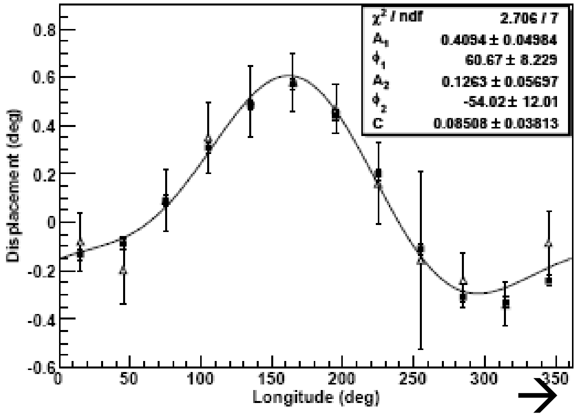

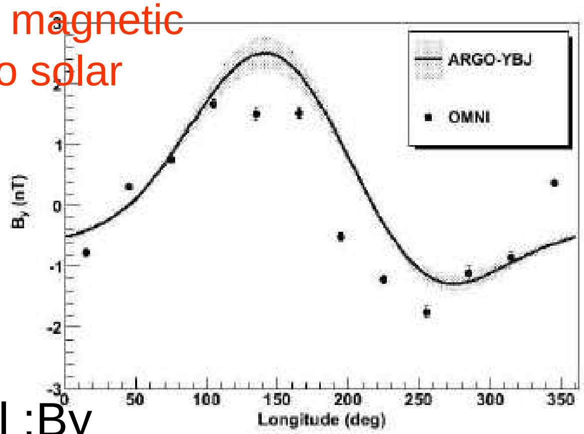

→ Parker model :By near the earth

→ time lag 1.6 days

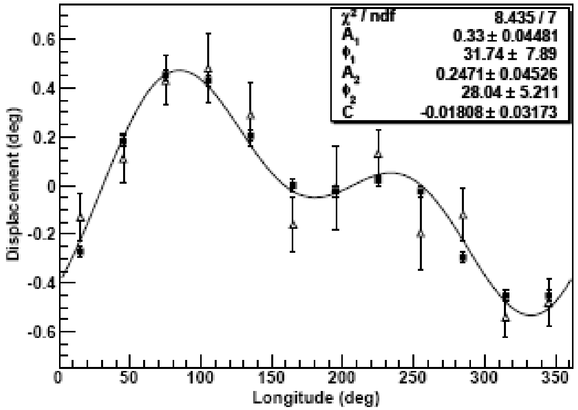

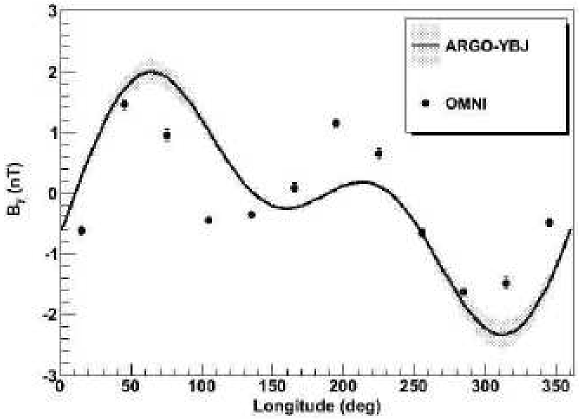

Fig.2. Shift of the centre of the sun shadow along the north-south direction during a complete Carrington period. The horizontal axis gives the Carrington longitude and the vertical axis is the angular displacement of the centre of the shadow. In the upper panel, the observation (triangles) in the period G_1 reveals that the shadow walks towards north in nearly half of the Carrington period and towards south in the rest of the period. The curve is a fit with a harmonic functional form. Squares represent the displacements of the simulated sun shadows. In the lower panel, a similar shift of the shadow but with different pattern is observed in period G_2, i.e. the shadow moves from side to side twice per Carrington period.

Fig.3. Comparison between two measurements of IMF using different methods. The solid curve represents the field component B_y near the earth measured by the ARGO-YBJ experiment using cosmic ray deflection. In period G_1 (upper panel) a clear bisector pattern is observed. Positive sign indicates that the field is pointing to the centre of the sun. An uncertainty of one standard deviation is marked by the shaded area. Solid dots represent the measurements using the OMNI observational data downloaded from [9]. In the lower panel, the results with the 4-sector structure in period G_2 are displayed.

Large Scale Anisotropy

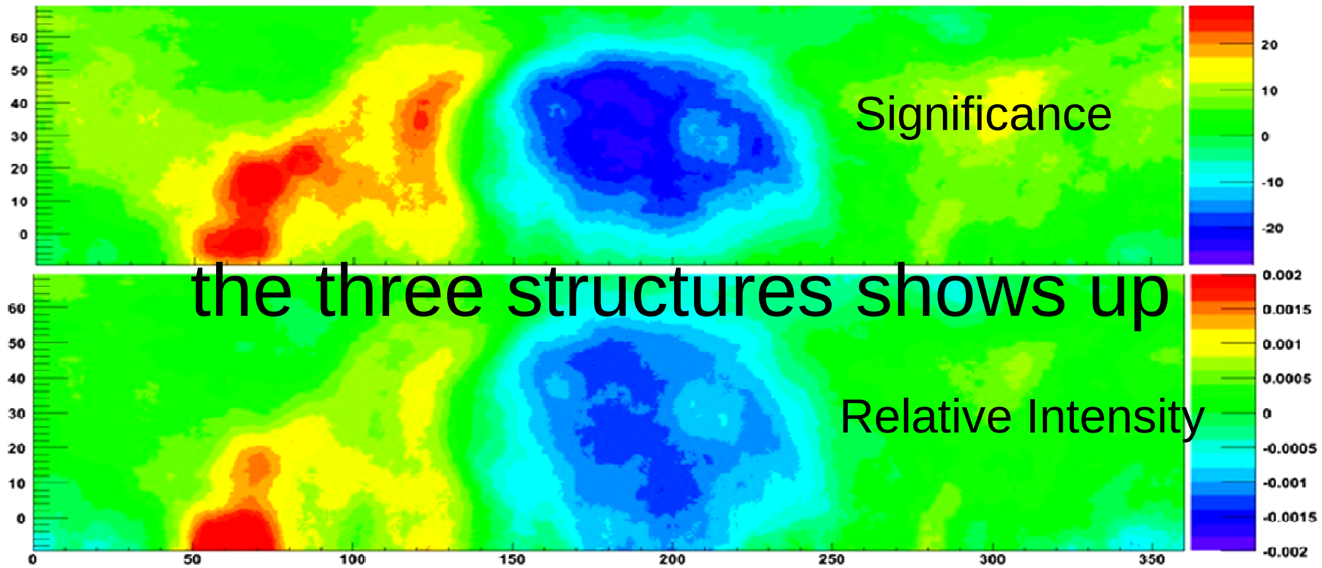

the three structures shows up

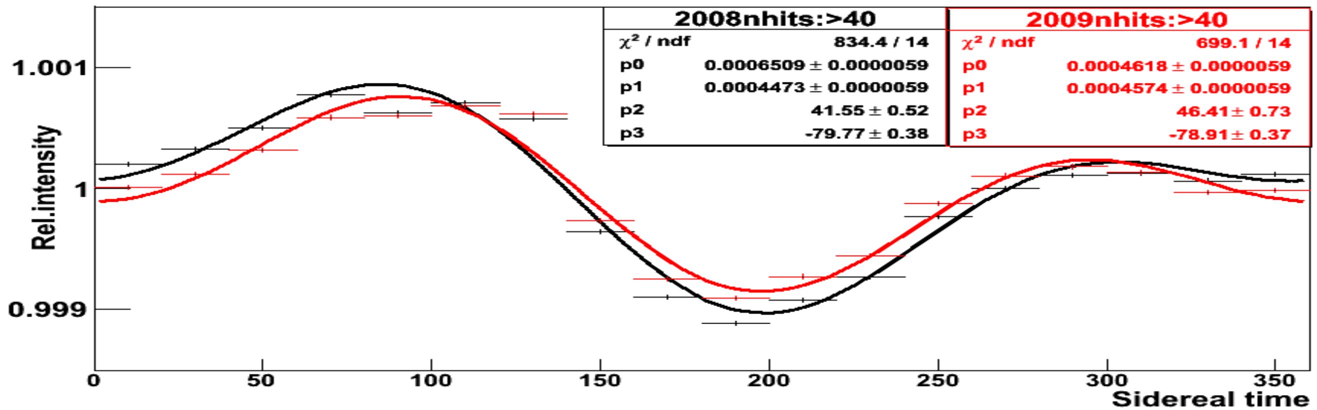

two year’s stablility

January 2008 – December 2009

Npad>40

zenith<45°

Background estimated with the “all-distance equi-zenith method”

(iterative procedure sensitive to any angular scale)

LSA: Energy Dependence

0.9TeV
1.52TeV
2.41TeV
3.58TeV,
7.17TeV
12.47TeV
23.6TeV

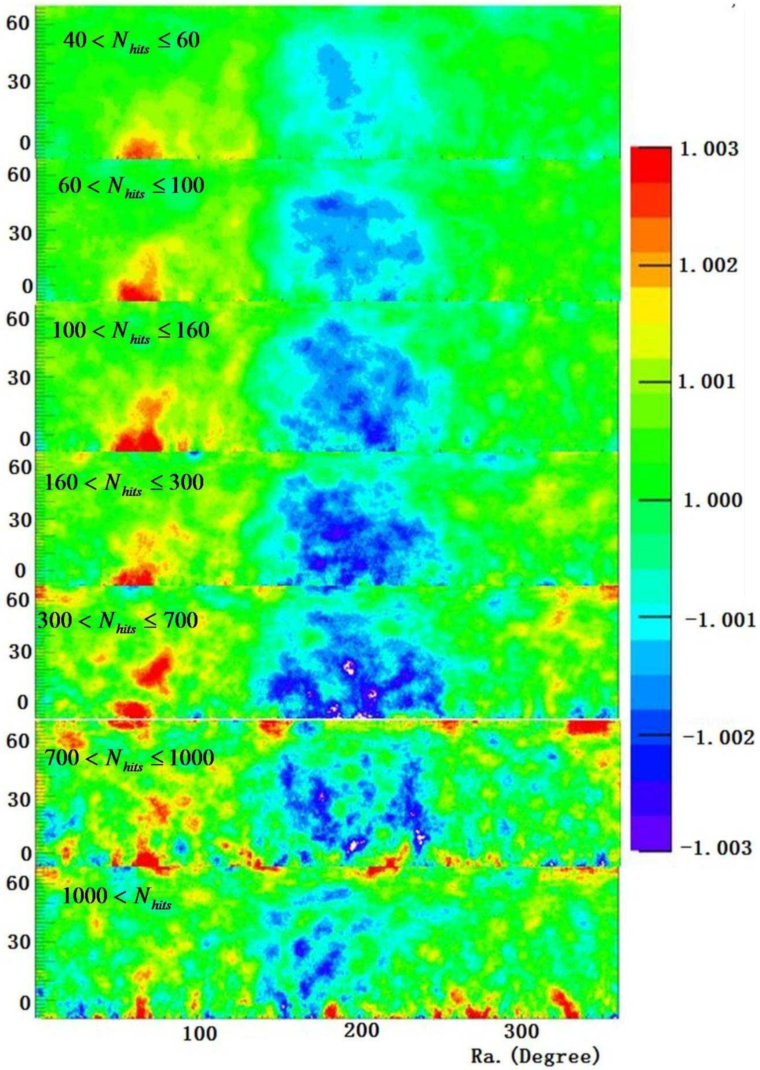

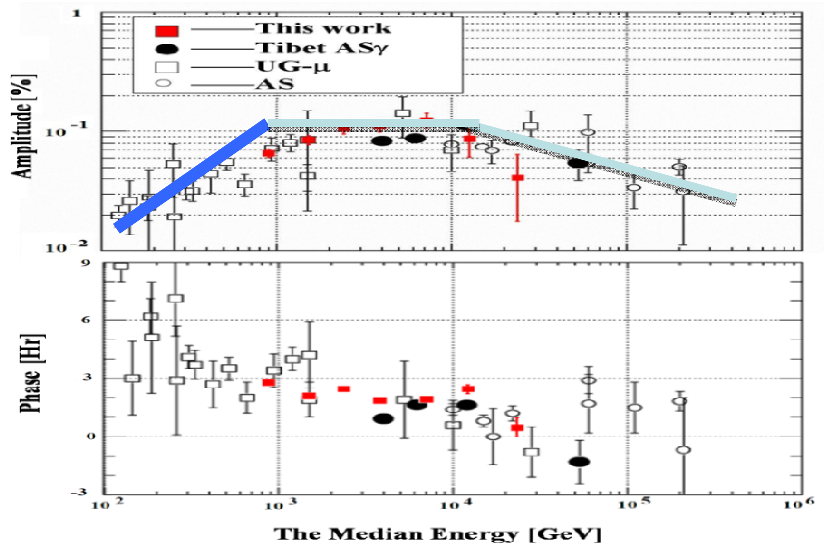

- **Scale:**
  faint — clear— faint
- **Energy Spectrum:**
  it is clear that change at around 10TeV
- **Phase :** stable

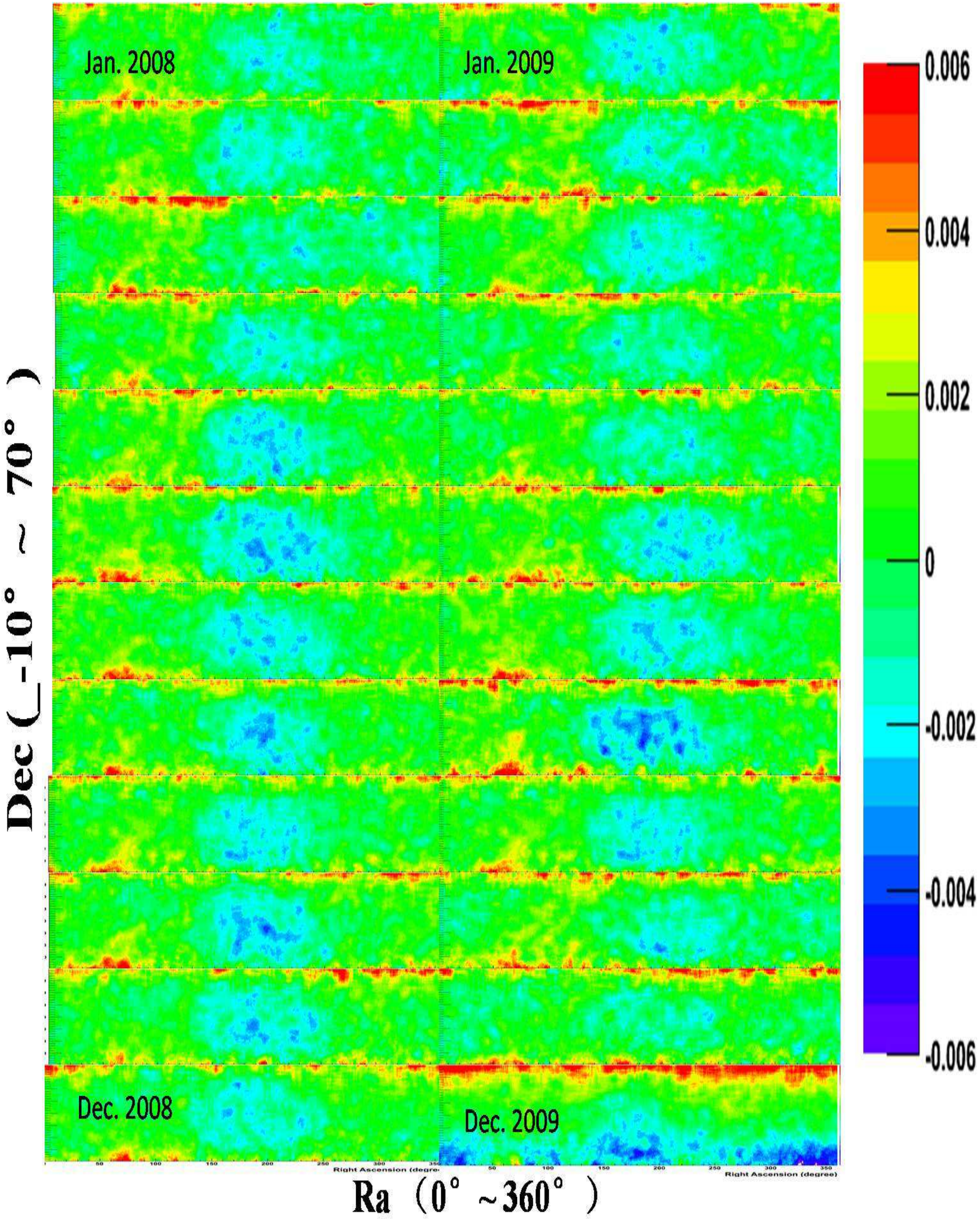

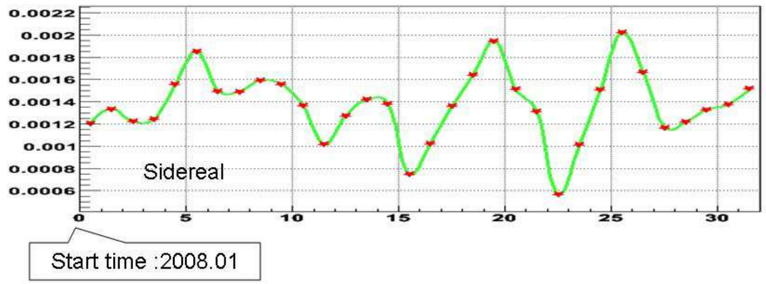

LSA: Monthly variation:ok

medium scale: significance map

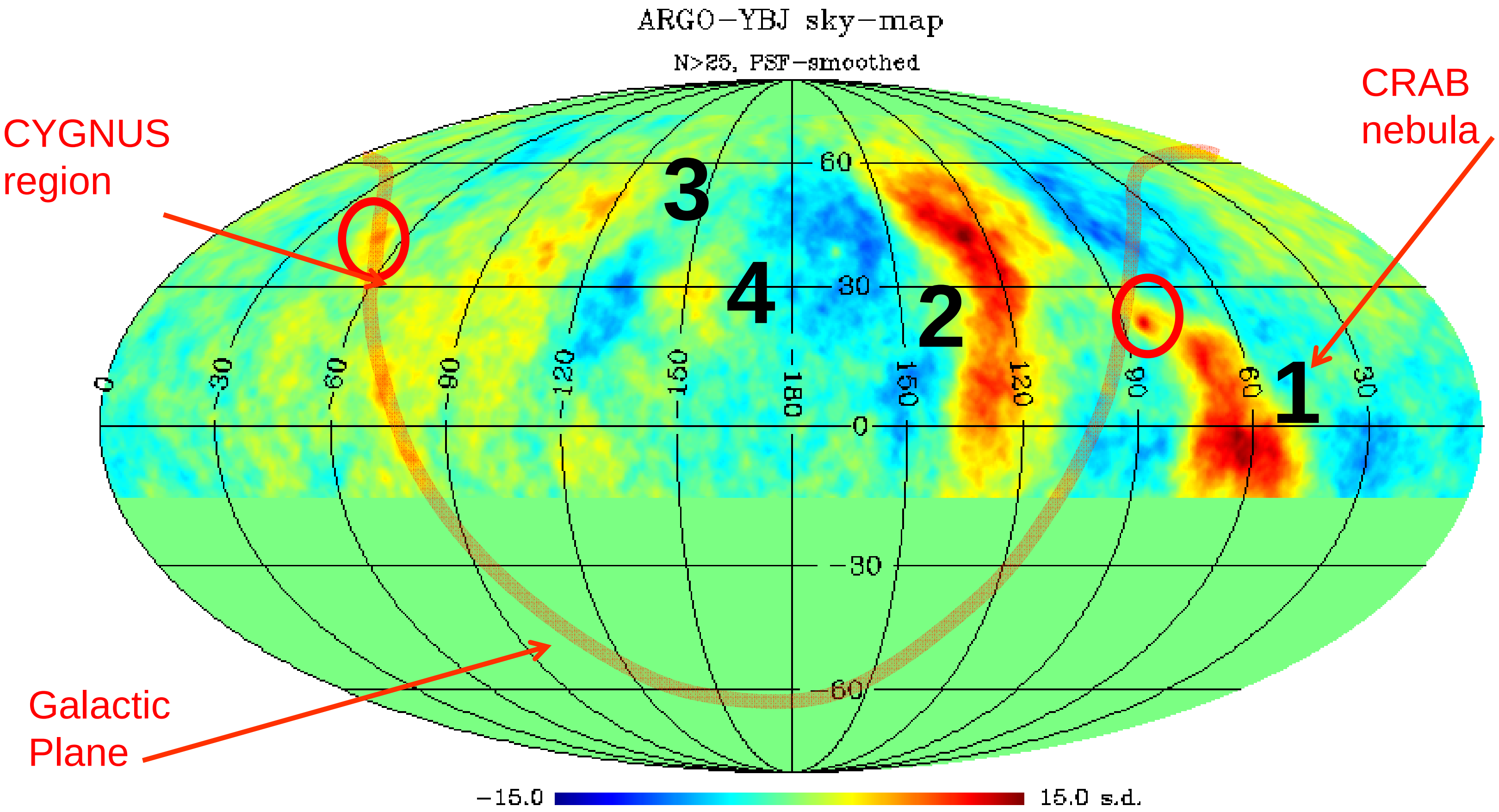

Map **smoothed with the detector P.S.F. for cosmic rays**

→no correction for trial factor is needed. If the "Top-Hat" smoothing is used and the optimal opening angle is looked for, the pre-trial maximum significance is 23 s.d.

→details on finer scales are not washed out by the Top-Hat function.

msa relative intensity map

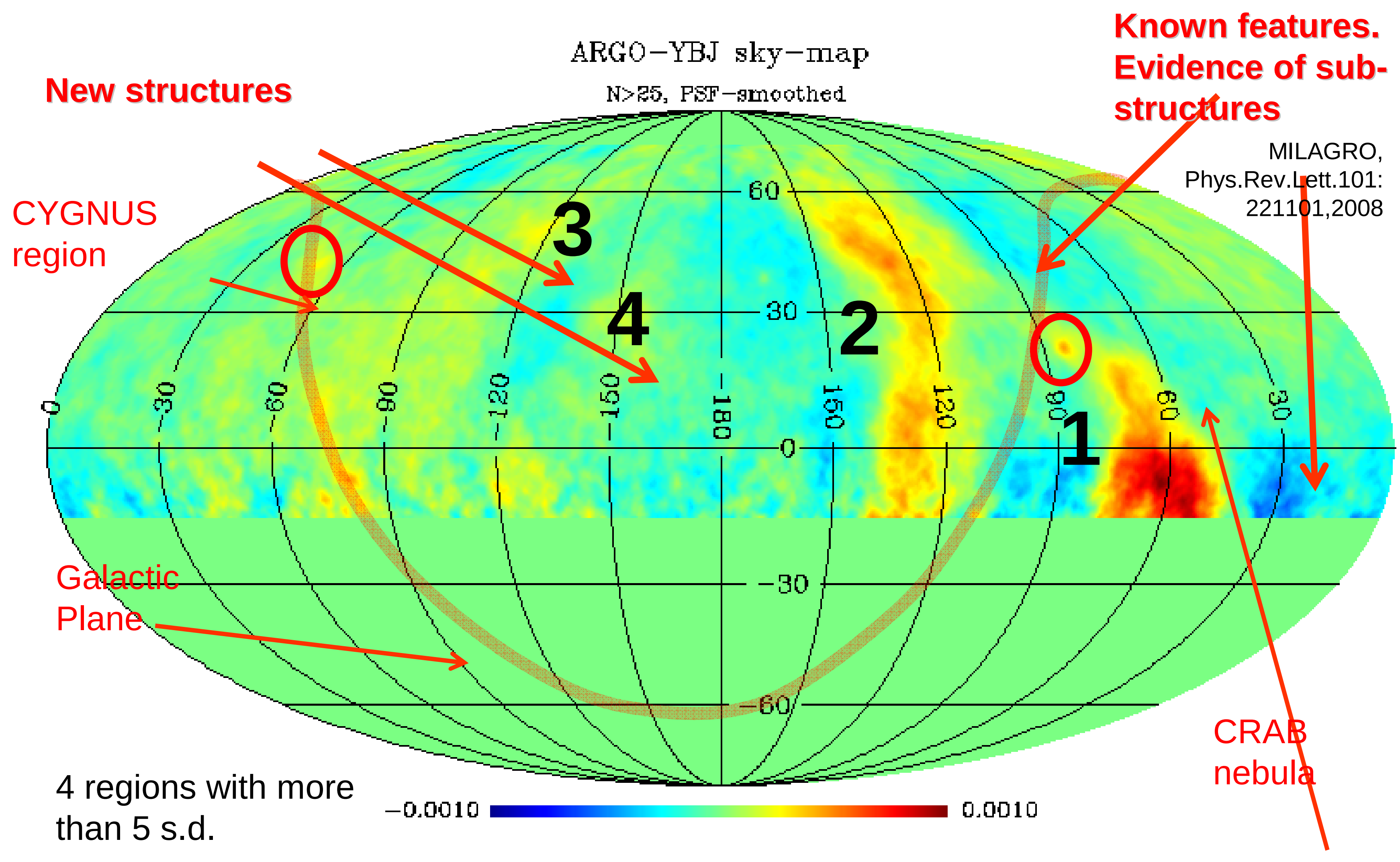

4 regions with more than 5 s.d.

Anisotropy : joint data

1. **All scale analysis is on going**. Started a collaboration with people in ICECUBE to perform a joint analysis: anisotropy map on both hemisphere.

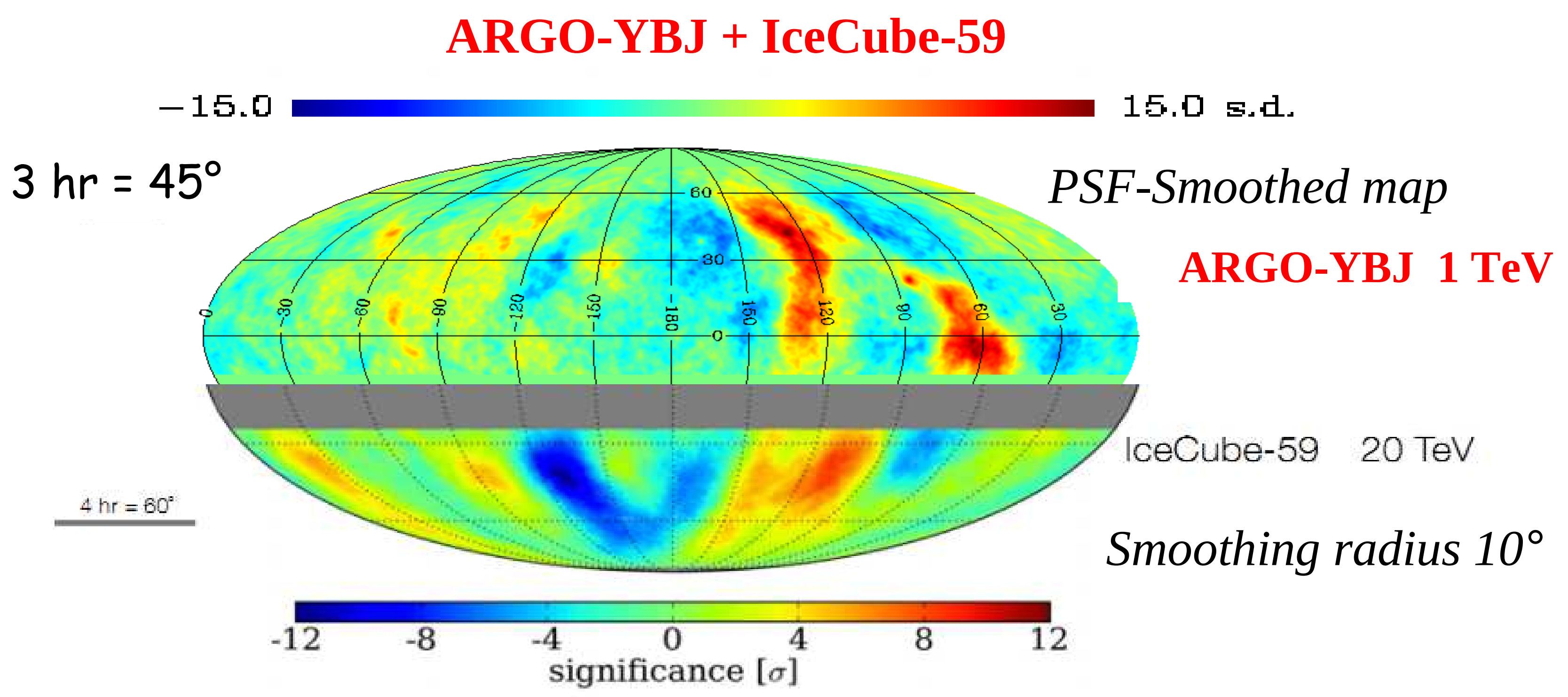

Proton-air cross section measurement

Use the shower frequency vs (secθ -1)

$$I(\theta) = I(0) \cdot e^{-\frac{h_o}{\Lambda}(\sec\theta - 1)}$$

for fixed energy and shower age.

The lenght Λ is not the p interaction lenght mainly because of collision inelasticity, shower fluctuations and detector resolution.

It has been shown that **Λ = k** λ_{int} , where k is determined by simulations and depends on:

- **hadronic interactions**
- **detector features and location (atm. depth)**
- **actual set of experimental observables**
- **analysis cuts**
- **energy, ...**

Then: **$\sigma_{p\text{-}Air}$ (mb) = 2.4 10^4 / λ_{int}(g/cm²)**

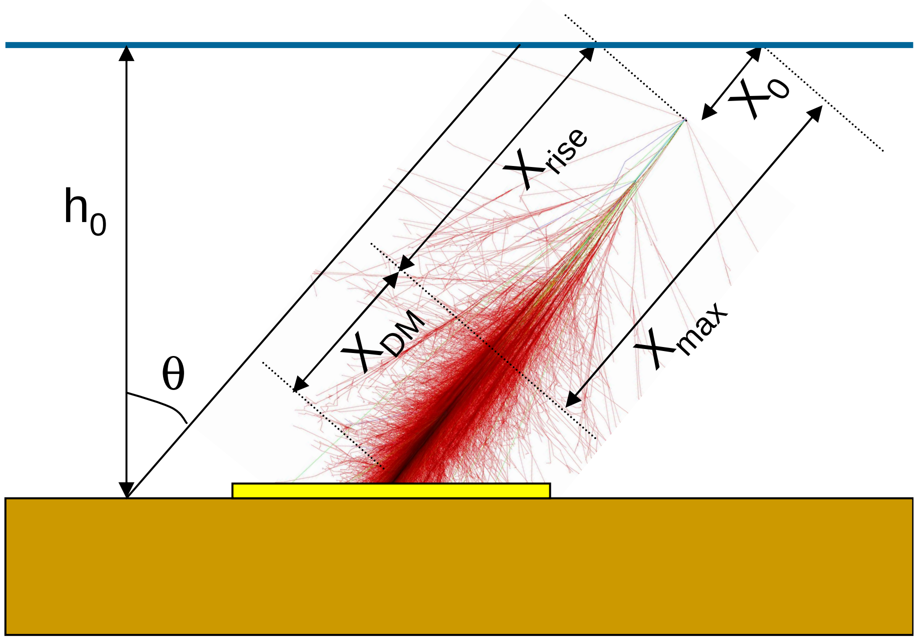

Take care of shower fluctuations

- **Constrain** $X_{DO} = X_{det} - X_0$ or
  $X_{DM} = X_{det} - X_{max}$
- **Select** deep showers (large X_{max}, i.e. small X_{DM})
- **Exploit** detector features (space-time pattern) and location (depth).

The proton-air cross section

ARGO-YBJ Coll.

Phys. Rev D 80, 092004 (2009)

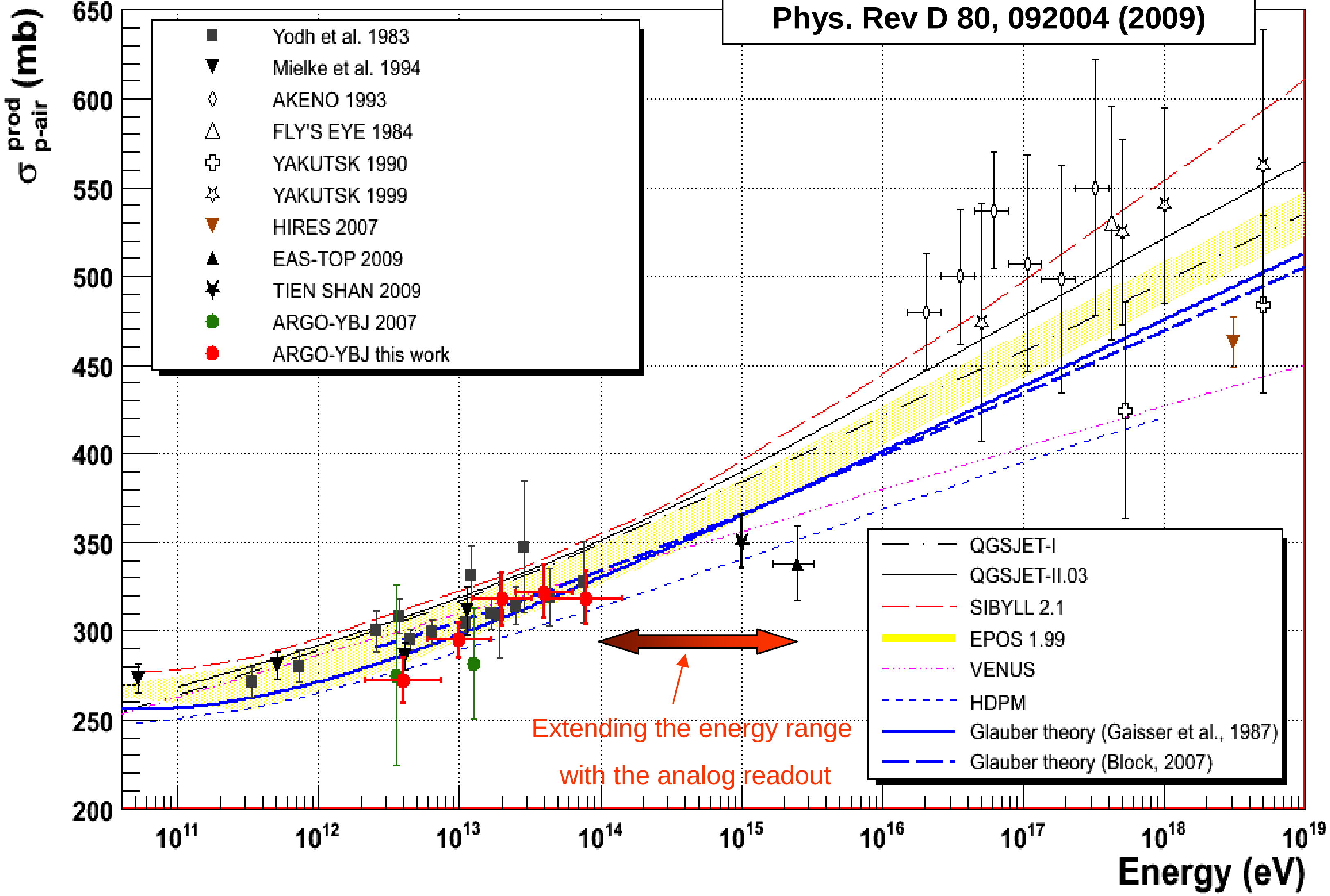

The total p-p cross section

- No p-p (and pbar-p) accelerator data available at these energies
- The $\log^2(s)$ asymptotic behaviour is favoured

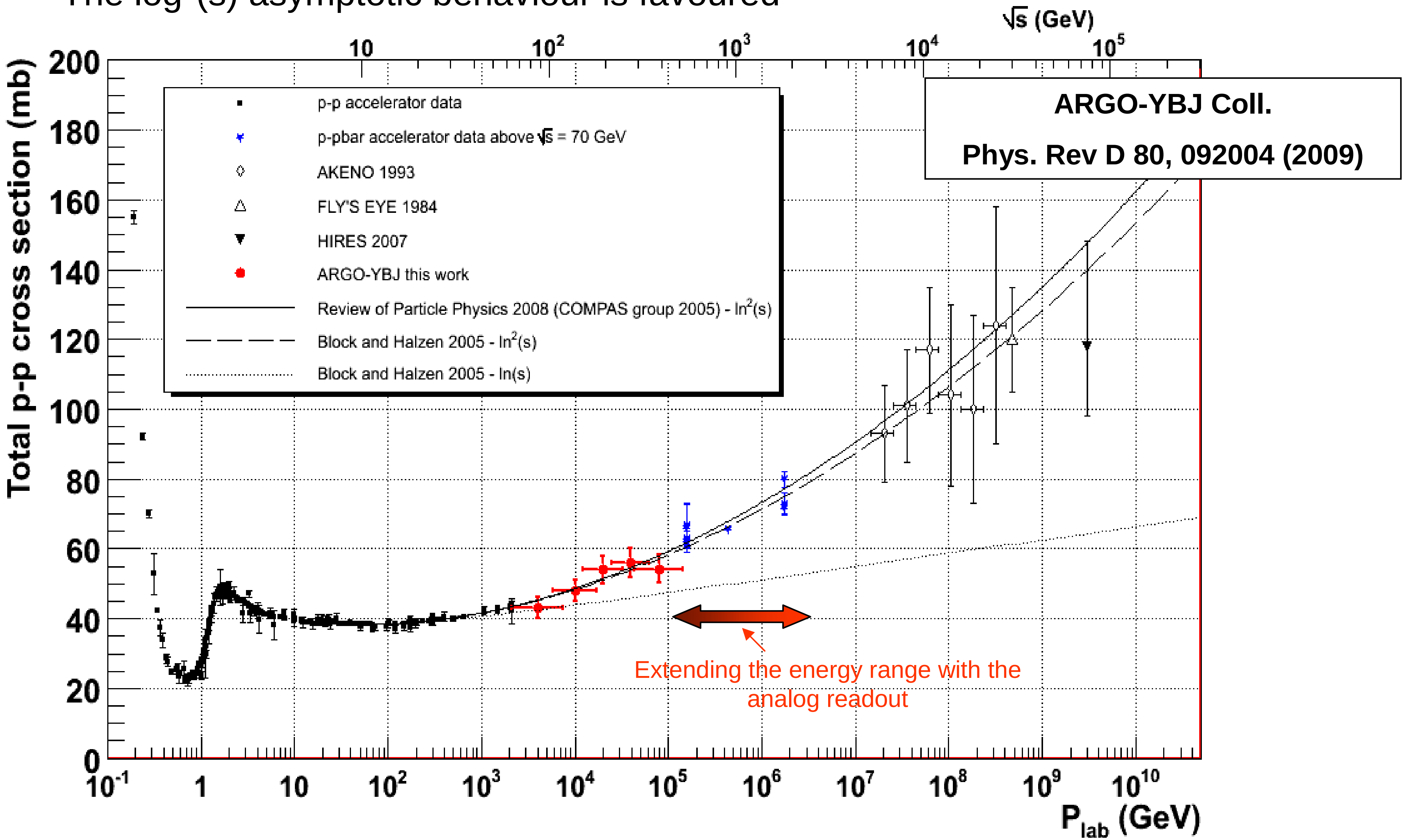

The CR light component energy spectrum

Unfolding the energy spectrum by a Bayesian approach

PRD 85, 092005 (2012)

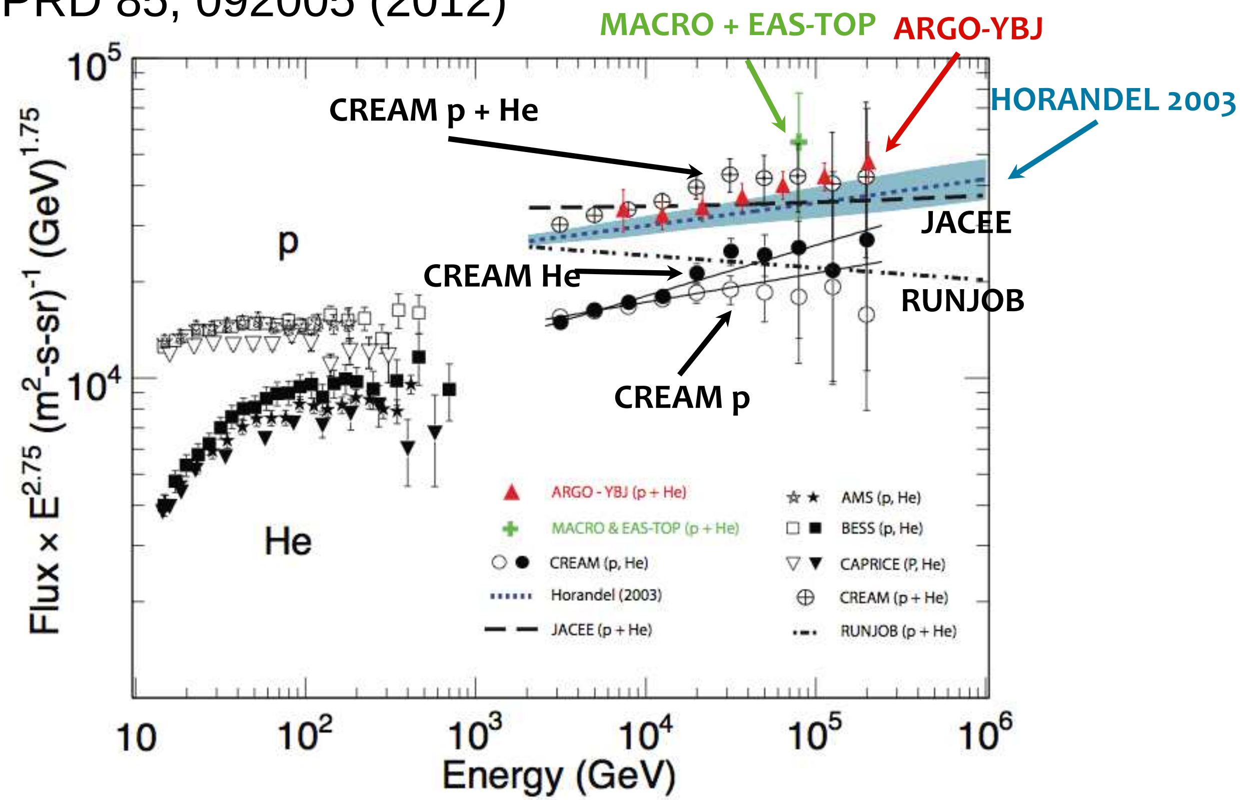

For the first time direct-indirect measurements of the CR spectrum overlaps for more than one energy decade, thus providing a solid anchorage to the CR spectrum measurements at higher energies.

The CR light component energy spectrum (1)

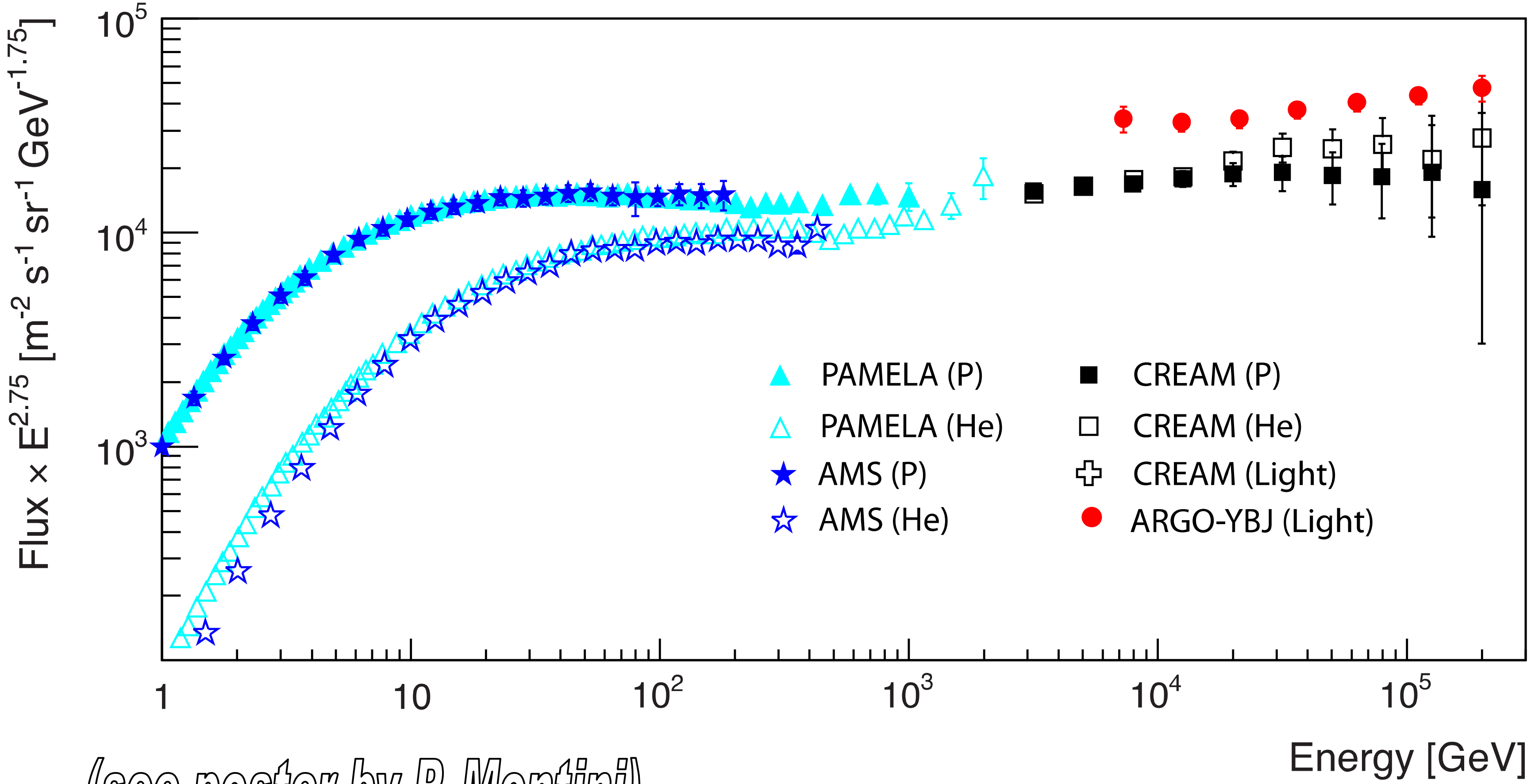

(see poster by P. Montini)

The CR light component energy spectrum(2)

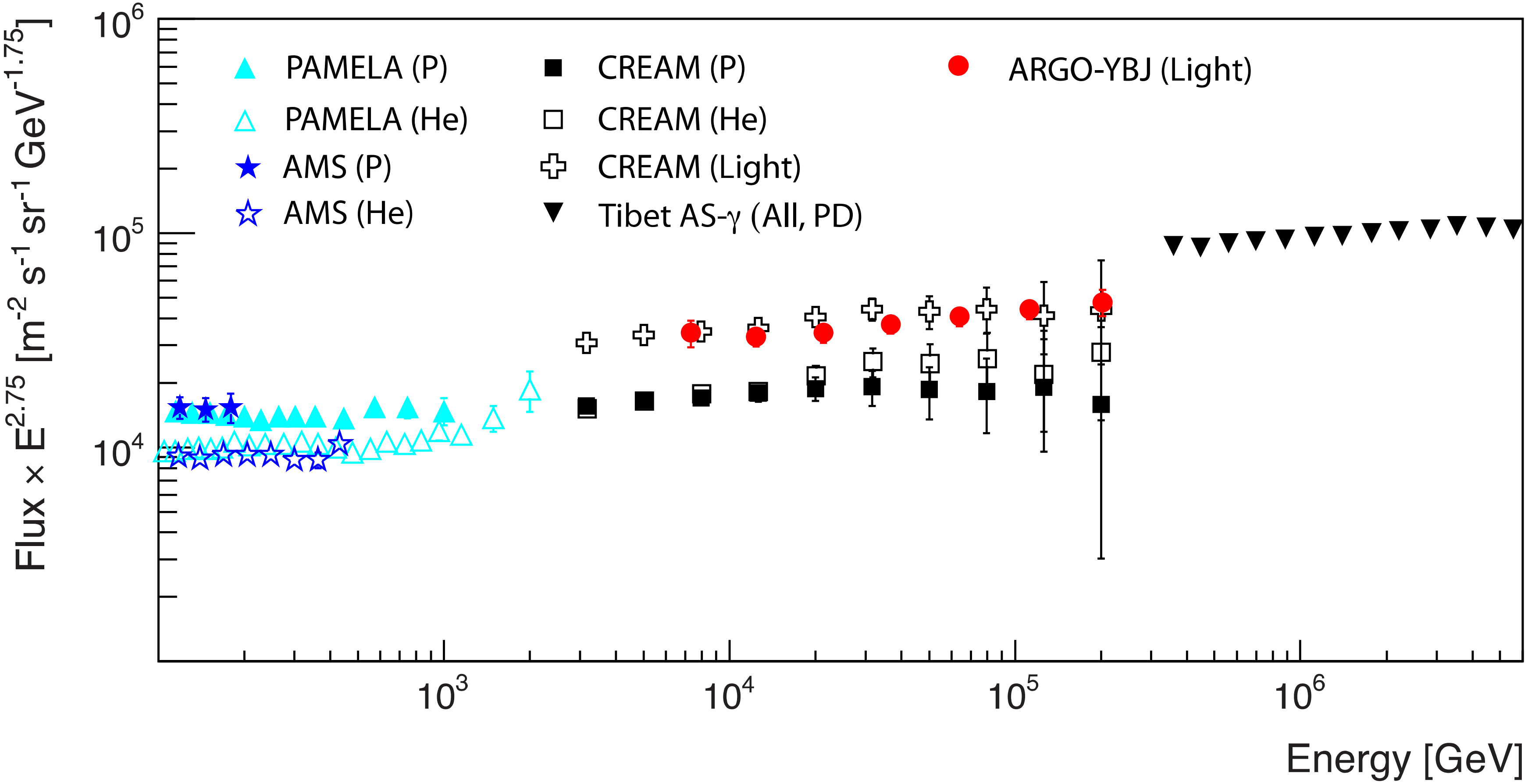

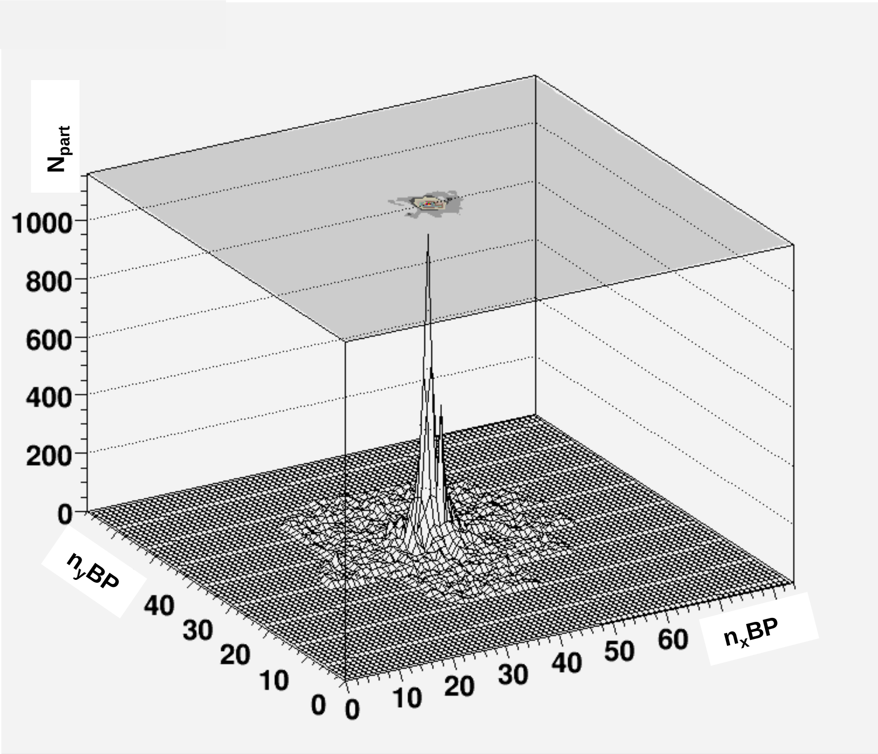

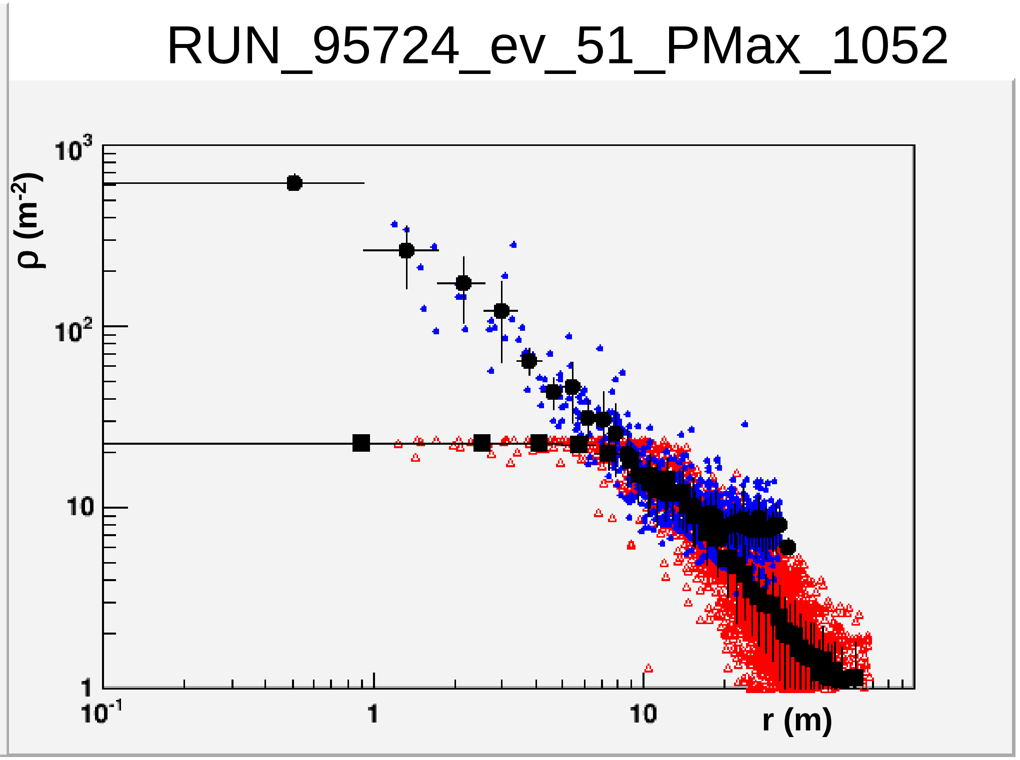

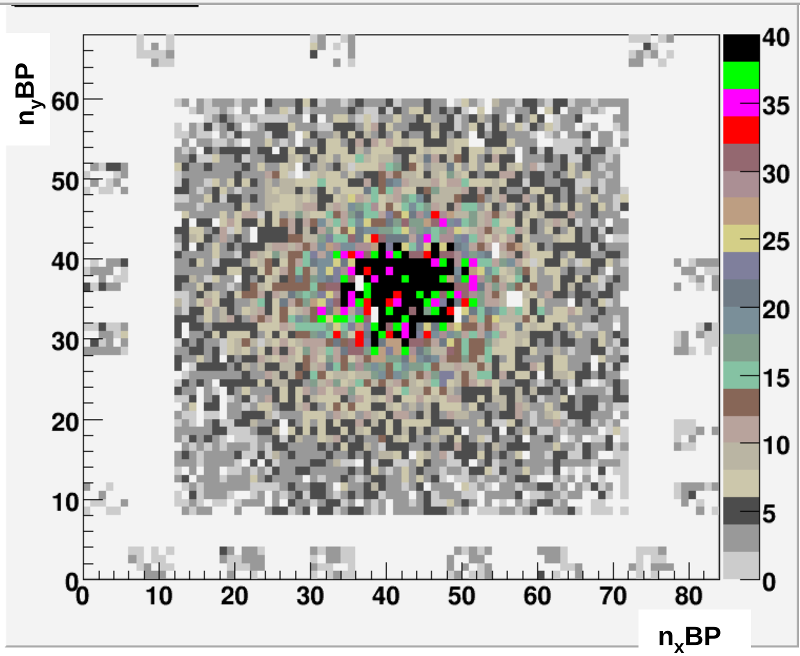

... above 100 TeV : Analog Readout

2.5 V fs

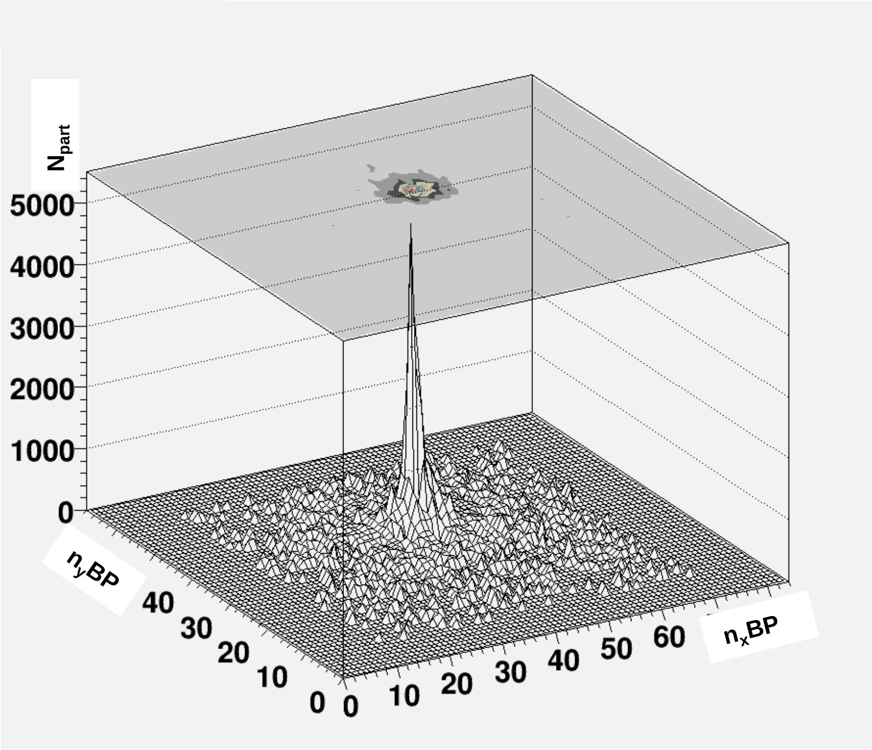

RUN_98177_ev_20_PMax_4998

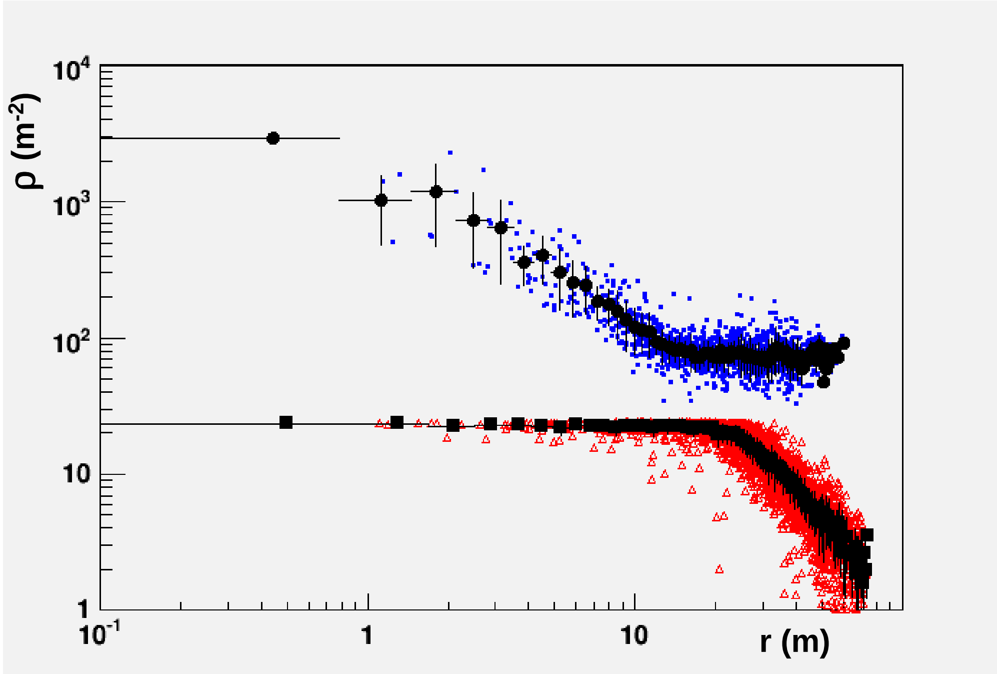

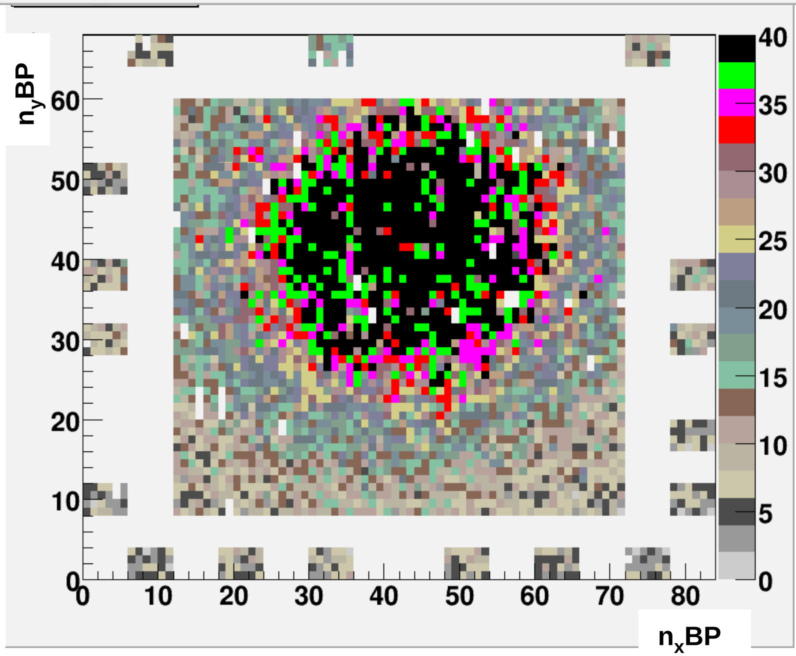

20 V fs

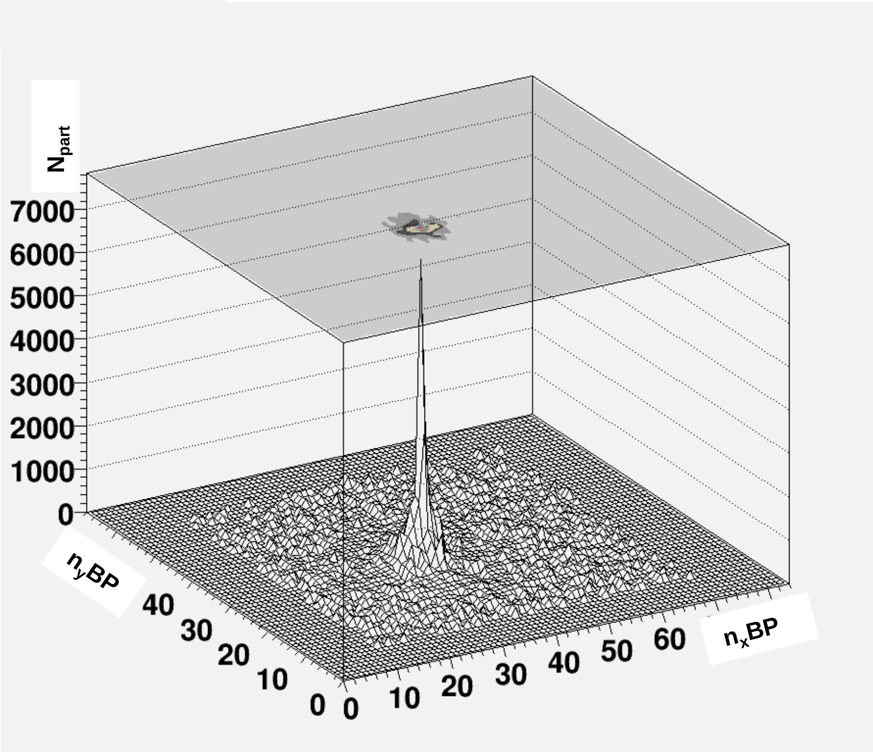

RUN_98175_ev_5_PMax_7110

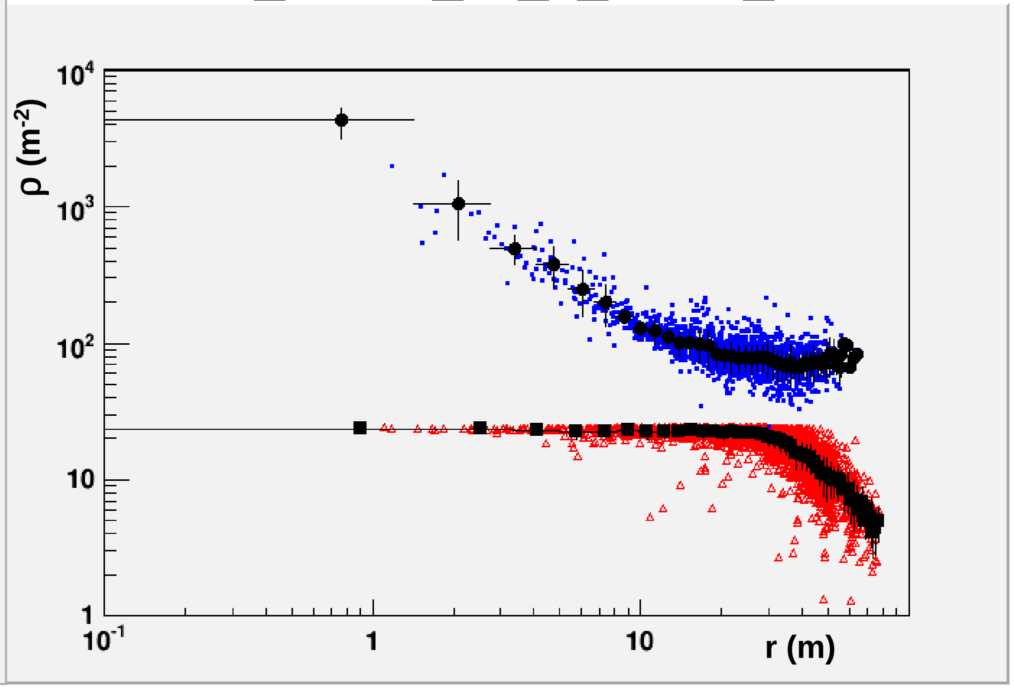

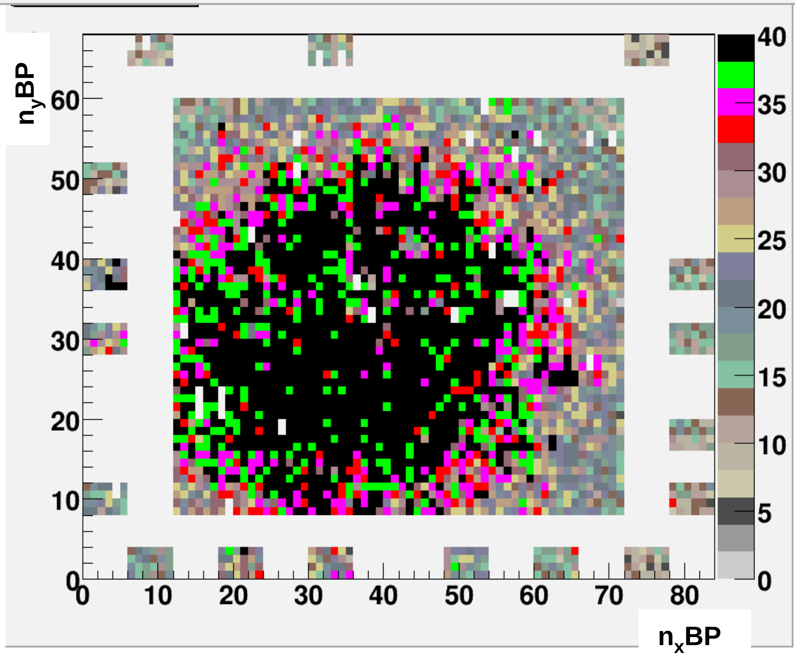

20 V fs

PMax : Shower Maximum

- ✓ 30% spread of the gain distribution (amplitude/particle)
- ✓ homogeneity ≈ 4 % (after calibration)

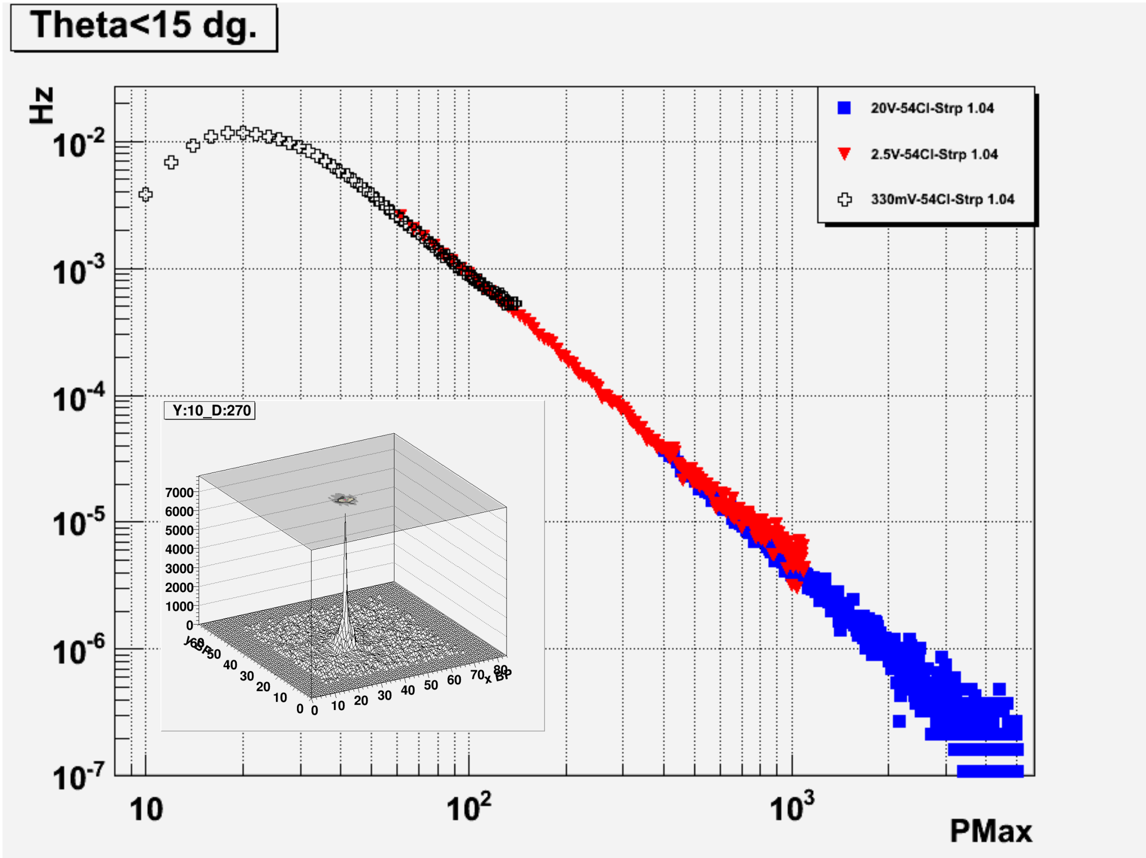

ARGO-YBJ data: PMax differential distribution

PMax in the shower

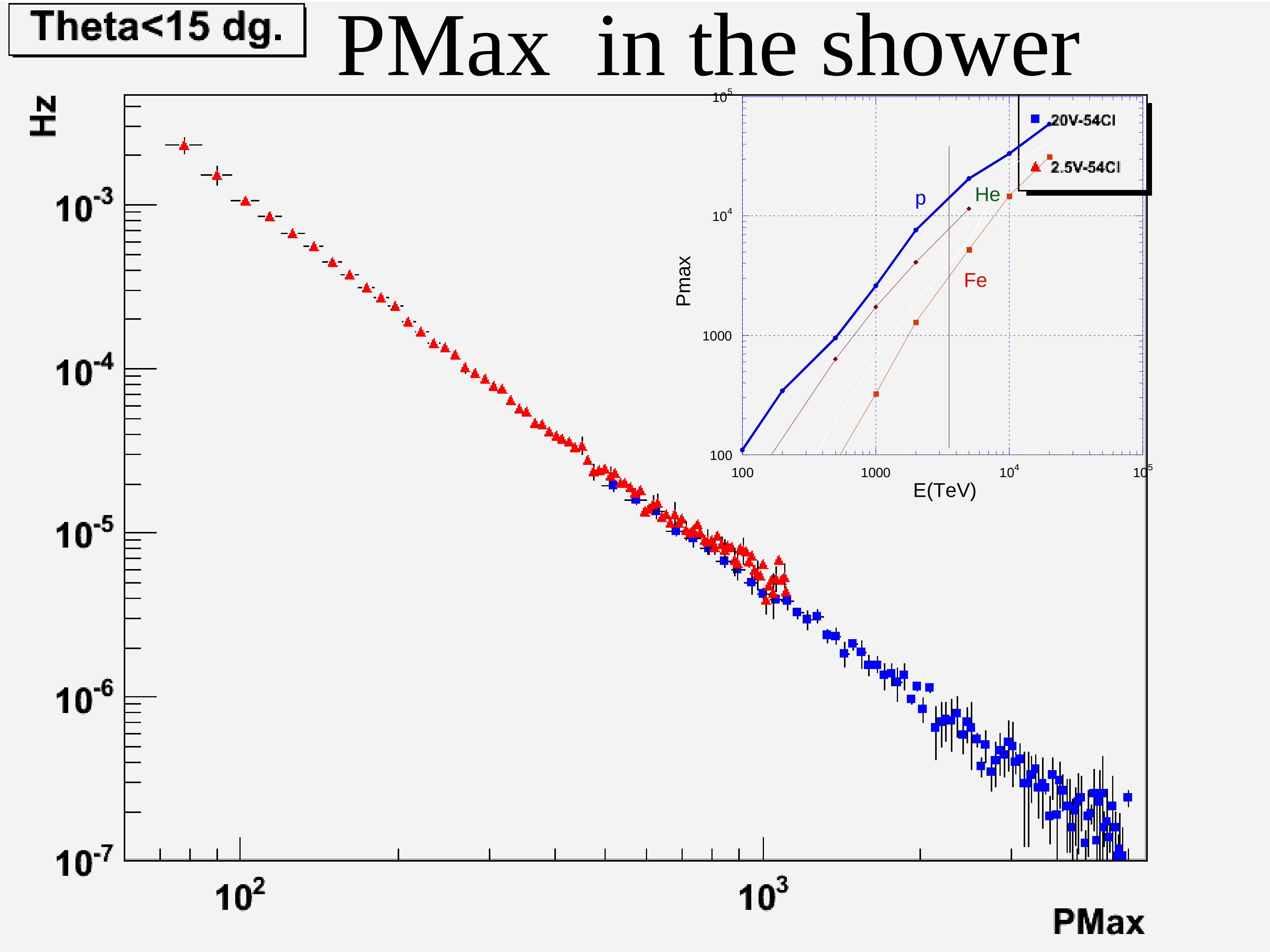

Tibet Array (4300 m asl)

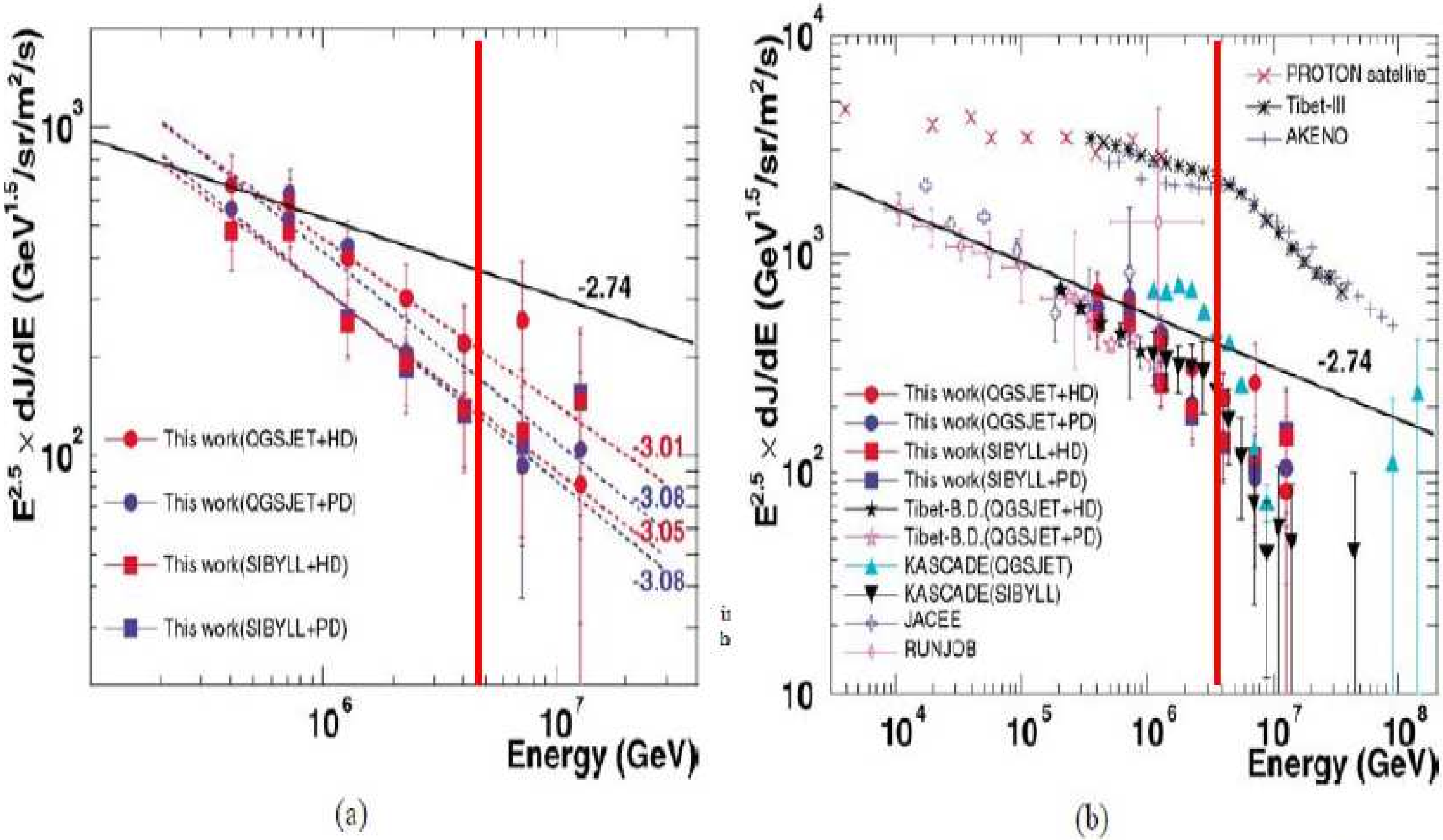

Fig. 2. Energy spectra of primary cosmic-ray protons obtained by the present experiment (a) and they are compared with other experiments (b): Tibet-B.D. [9], KASCADE [16], JACEE [17] and RUNJOB [18]. The all-particle spectra are from the experiments: PROTON satellite [19], Tibet-III [20] and AKENO [21]. For the solid line with the power index −2.74, see the text.

Lateral distribution

The core region is measured with unprecedented detail
→ Sensitivity to hadronization models/composition

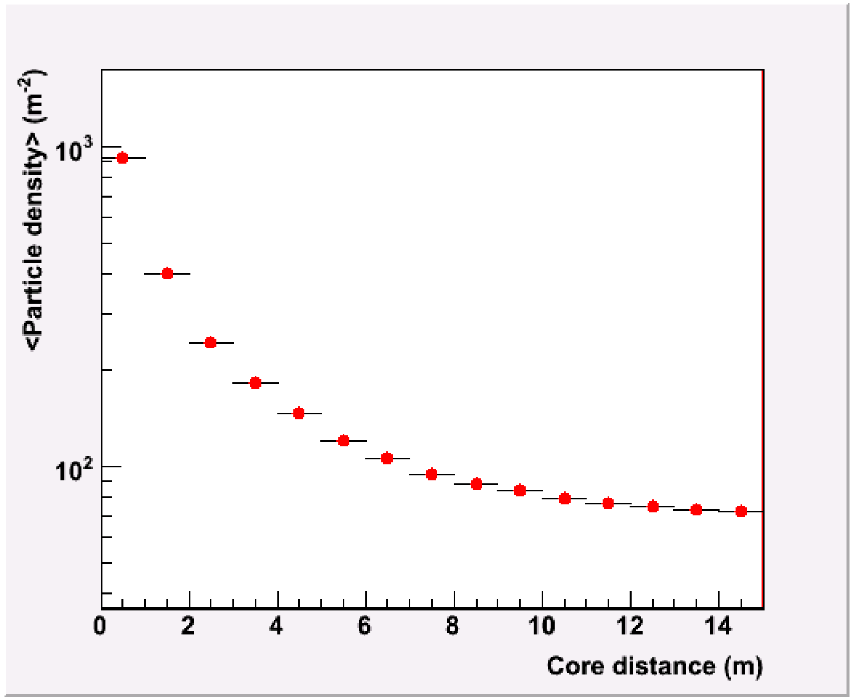

LDF per Npart_peak=(1-3) 10^3

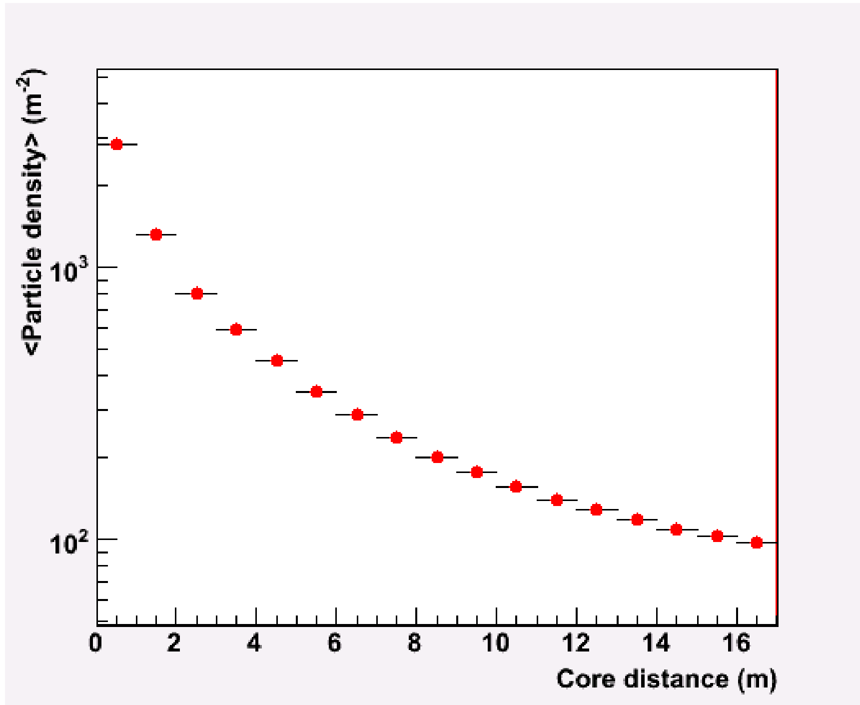

LDF per Npart_peak=(3-8) 10^3

Composition studies (1)

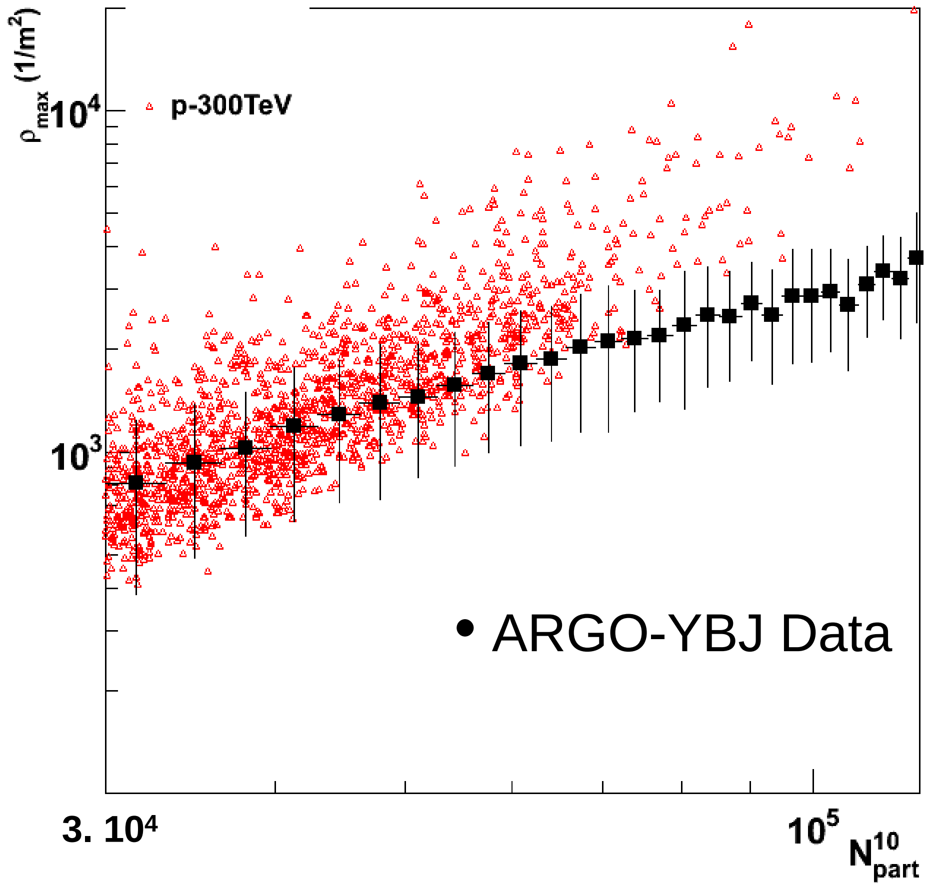

Composition studies (2)

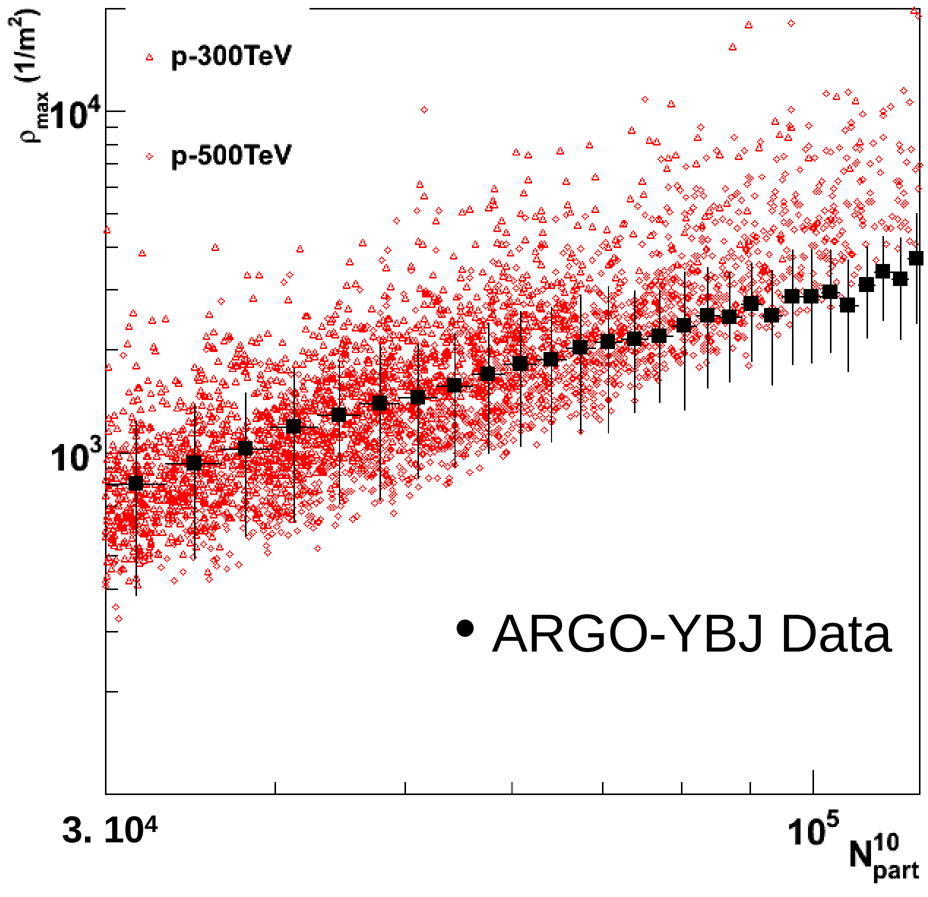

Composition studies (3)

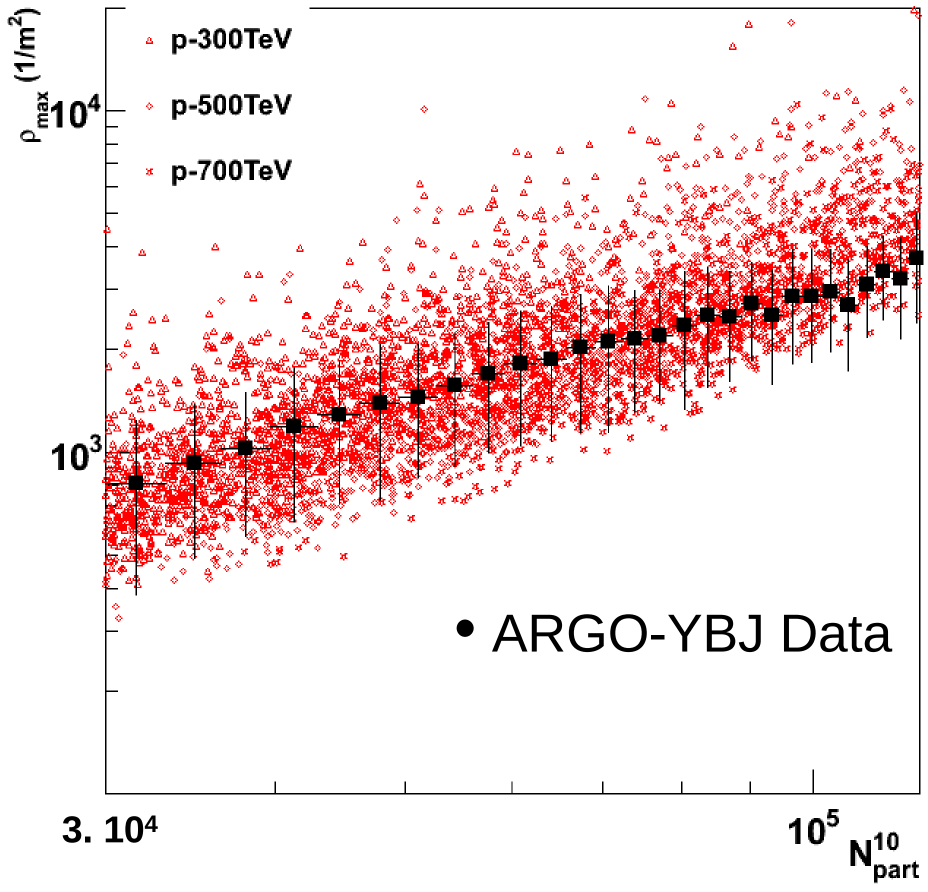

Composition studies (4)

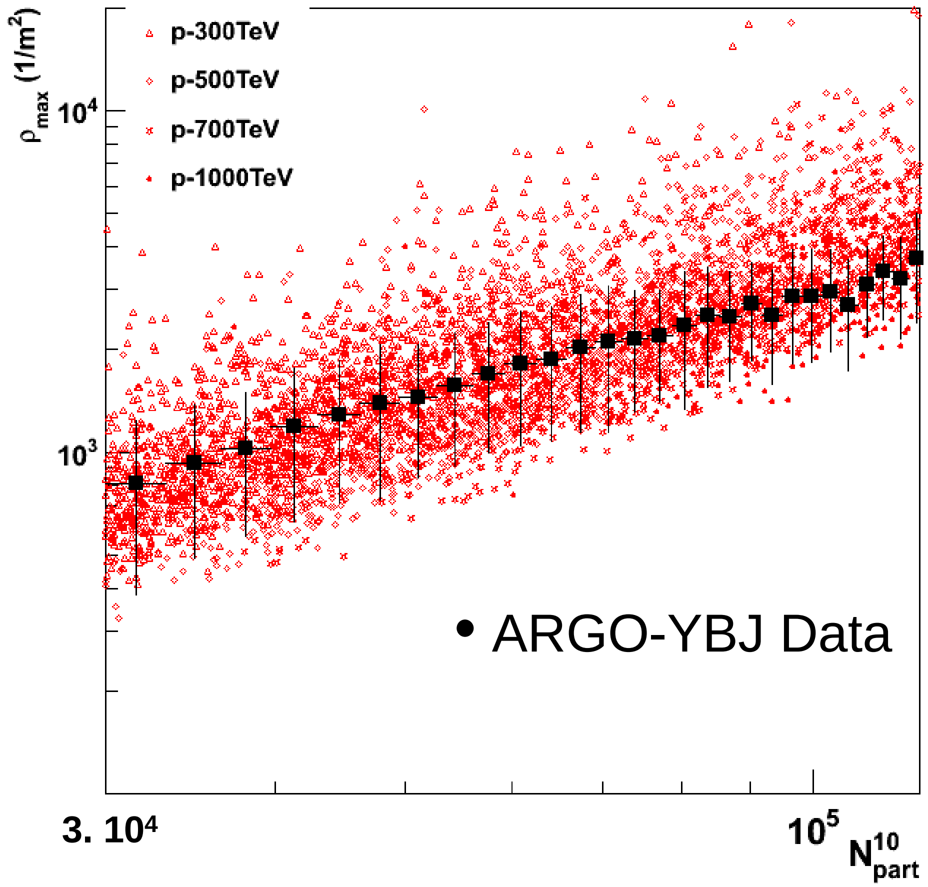

Composition studies (5)

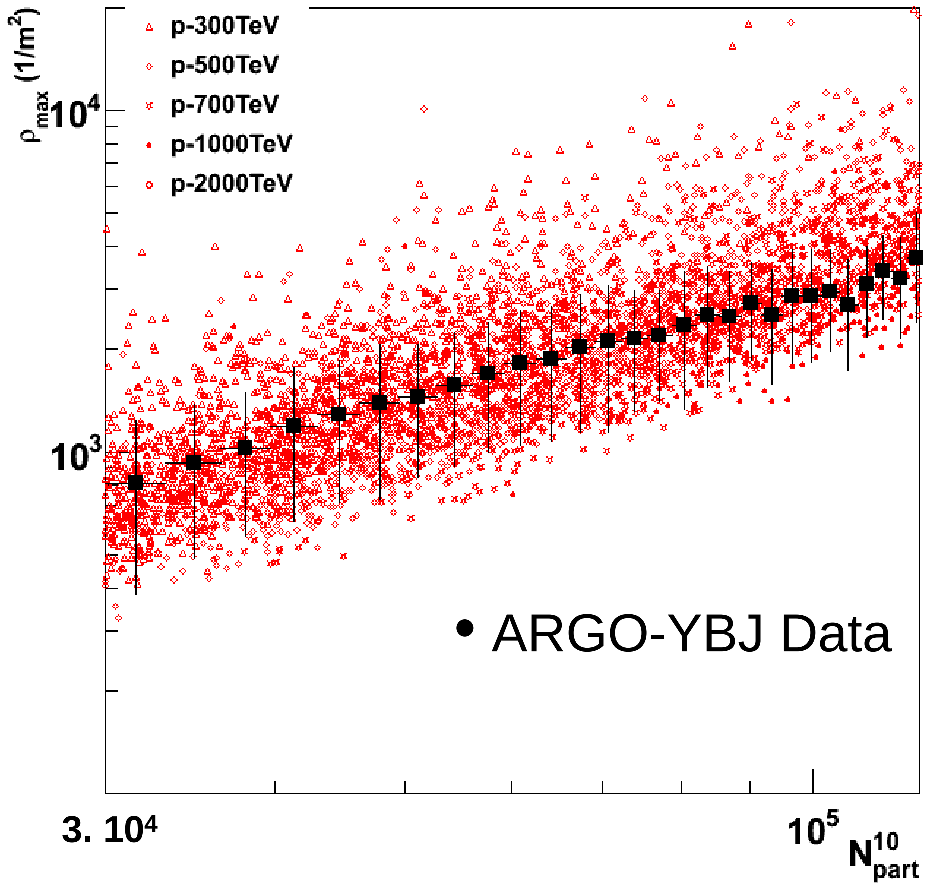

Composition studies (6)

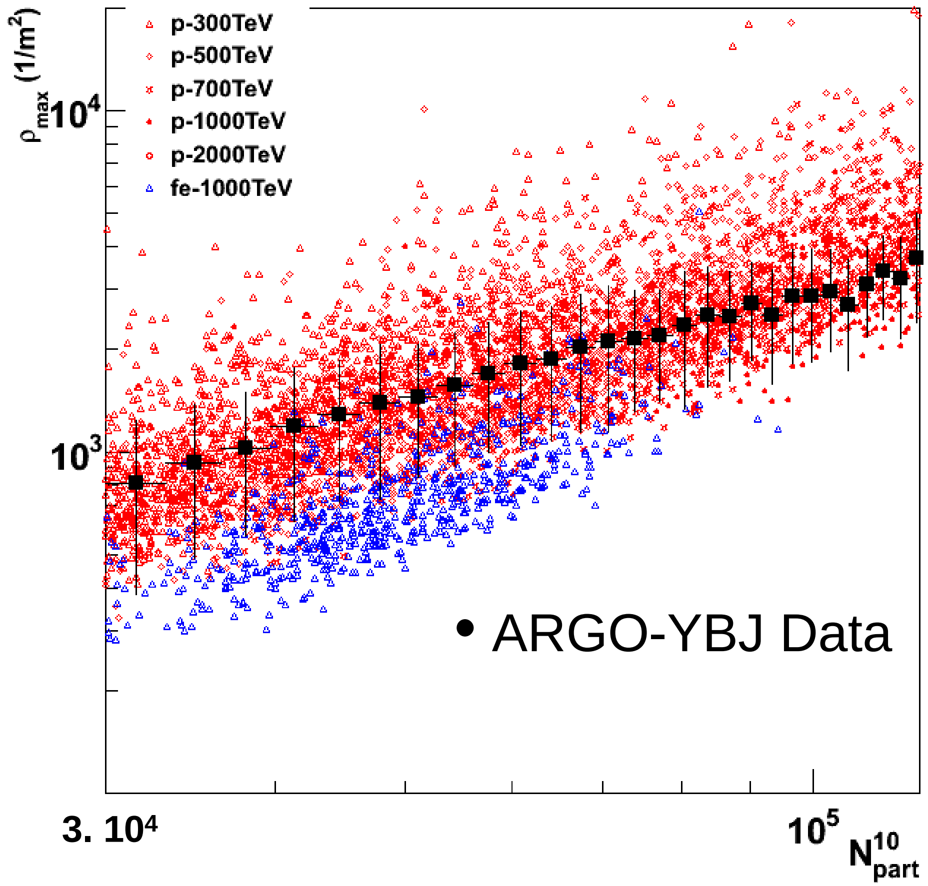

Composition studies (7)

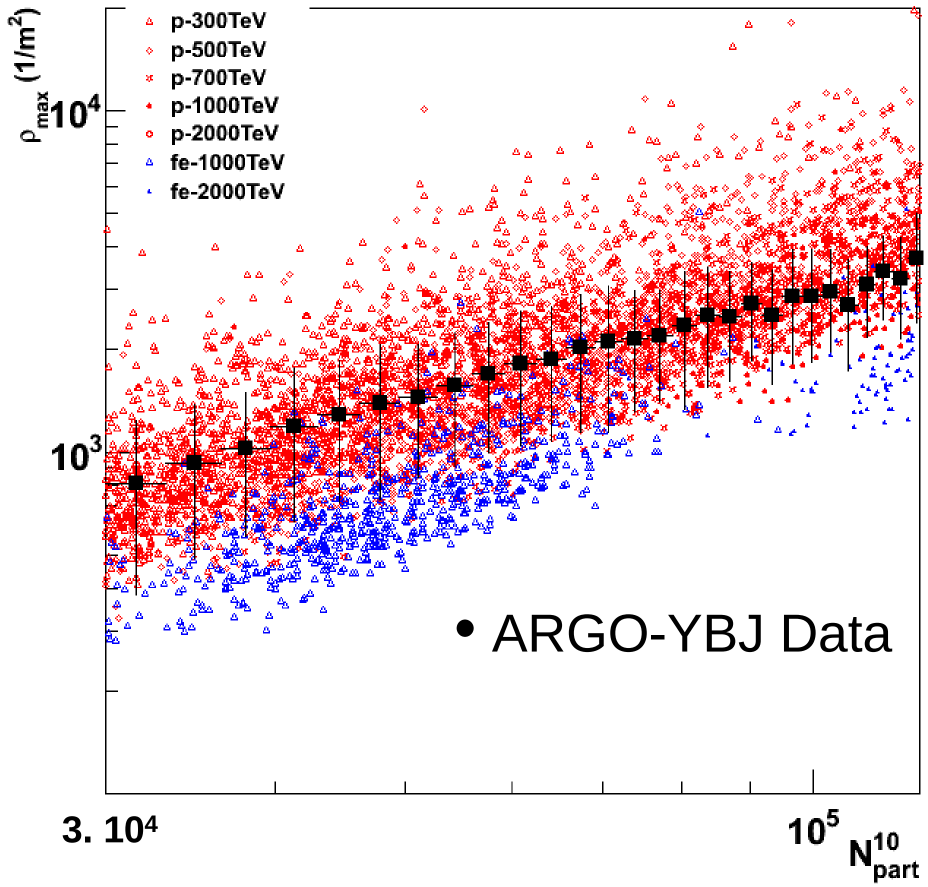

Composition studies (8)

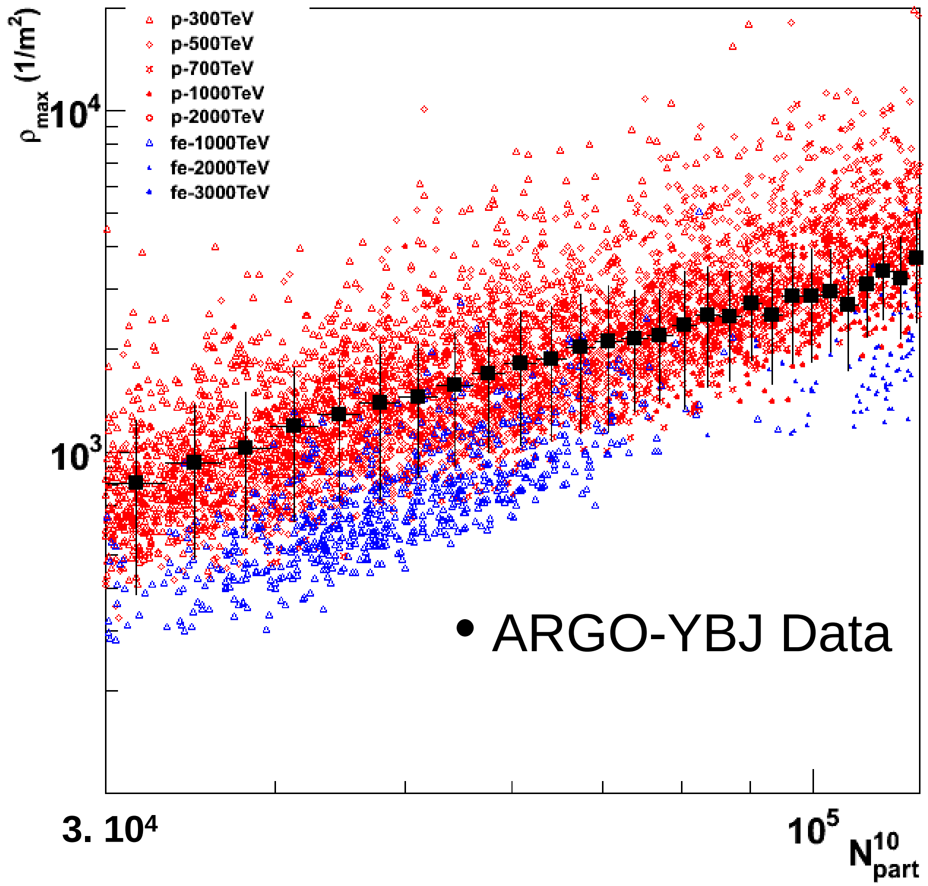

Event Asymmetry

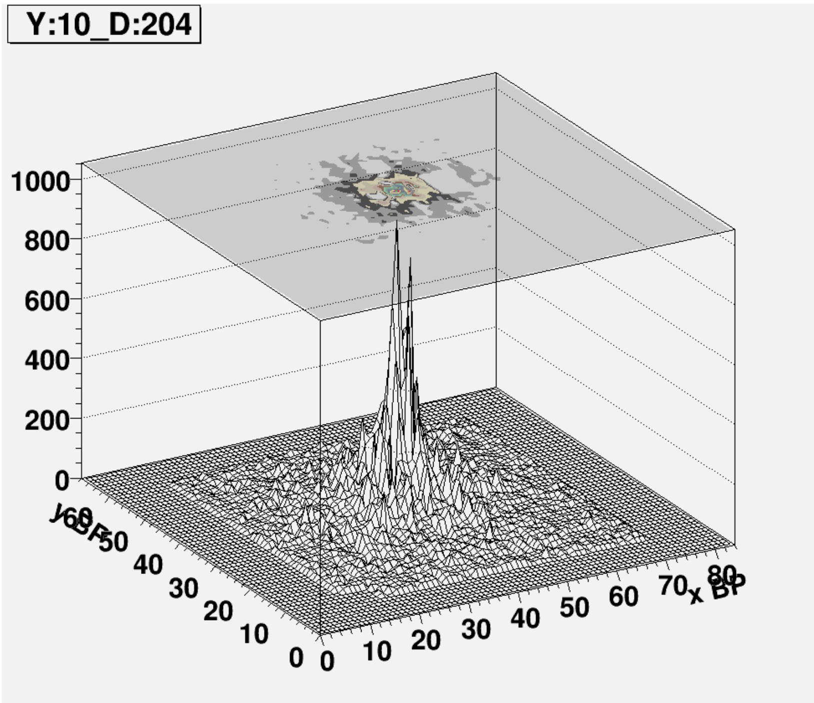

Events are selected by requiring:

- The reconstructed zenith angle is less than 15◦;.
- core inside the internal detector (the 6 ×
  9 clusters in the center)
- log of the maximum density in 2.5 to 3
- data from Dec. 2010 to Mar. 2011 is used.
- comparison with MC events generated according to Horandel model

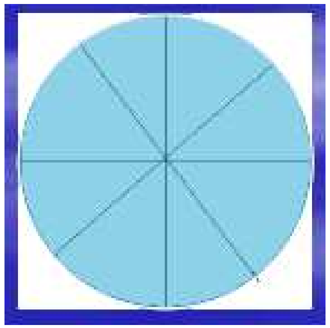

$$\xi = \frac{(Q_{\max} - Q_{\min})}{(Q_{\max} + Q_{\min})}$$

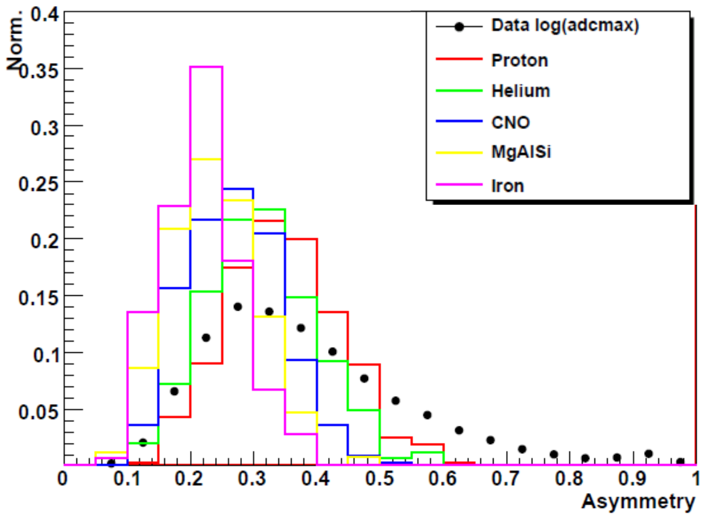

Asymmetry distribution :
comaparison of data and MC events

M. ZHA-ARGO-YBJ Coll., HE1.1 n.242

Multicore events

Those events are typically explained within the framework of jet production, which is essentially provided by the leading particle interaction with the Air target nuclei; the separation between the cores is related to the *pT* of the leading particle. Events at high *pT* are a perfect tool to investigate hadronic interaction models or even new physics.

- EAS data selection:
  hit strips > 5000,
  max ADC count > 10

- Multicore event selection :
  - significance > 5σ
  - r_{12} ~ 3.5 -10 m.

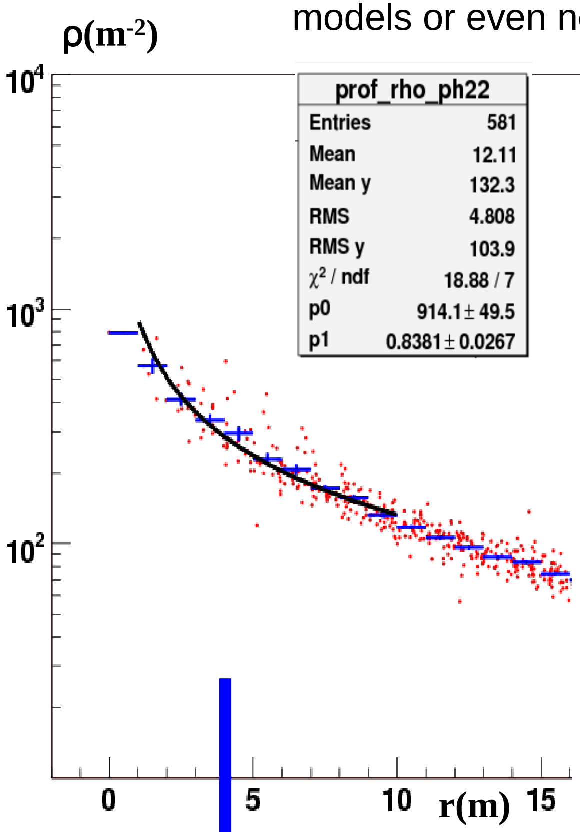

$$\rho(r) = C(s)\frac{N_e}{r_M^2}\left(\frac{r}{r_M}\right)^{s-2}\left(1+\frac{r}{r_M}\right)^{s-4.5}$$

$$\rightarrow \rho(r) = p_1 \cdot r^{p_2}$$

$$f = \lg\rho_{Meas}(r) - \lg\rho_{Fit}(r)$$

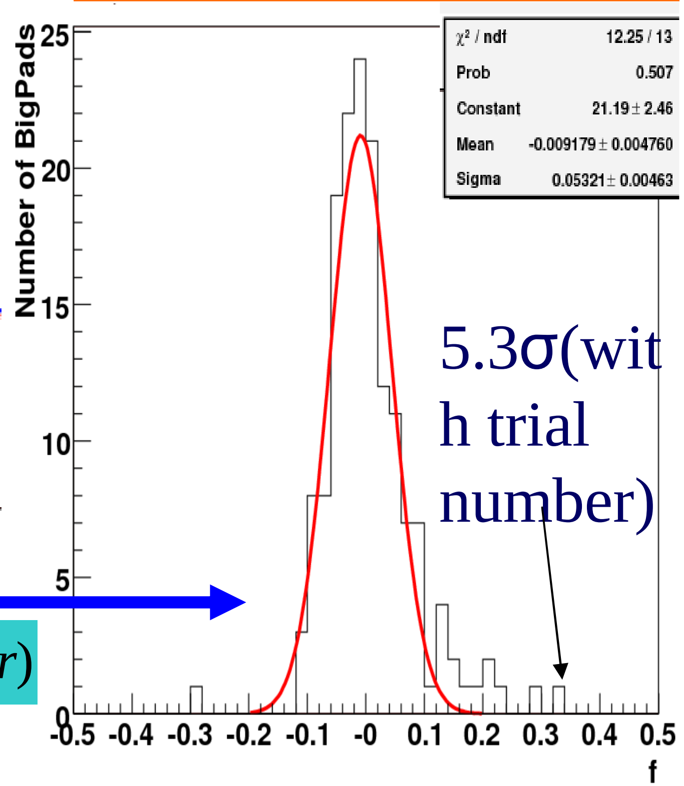

5.3σ(with trial number)

J. Zhao, X. Ma -ARGO-YBJ coll. ICRC2011- HE3.1 n.814

A real event

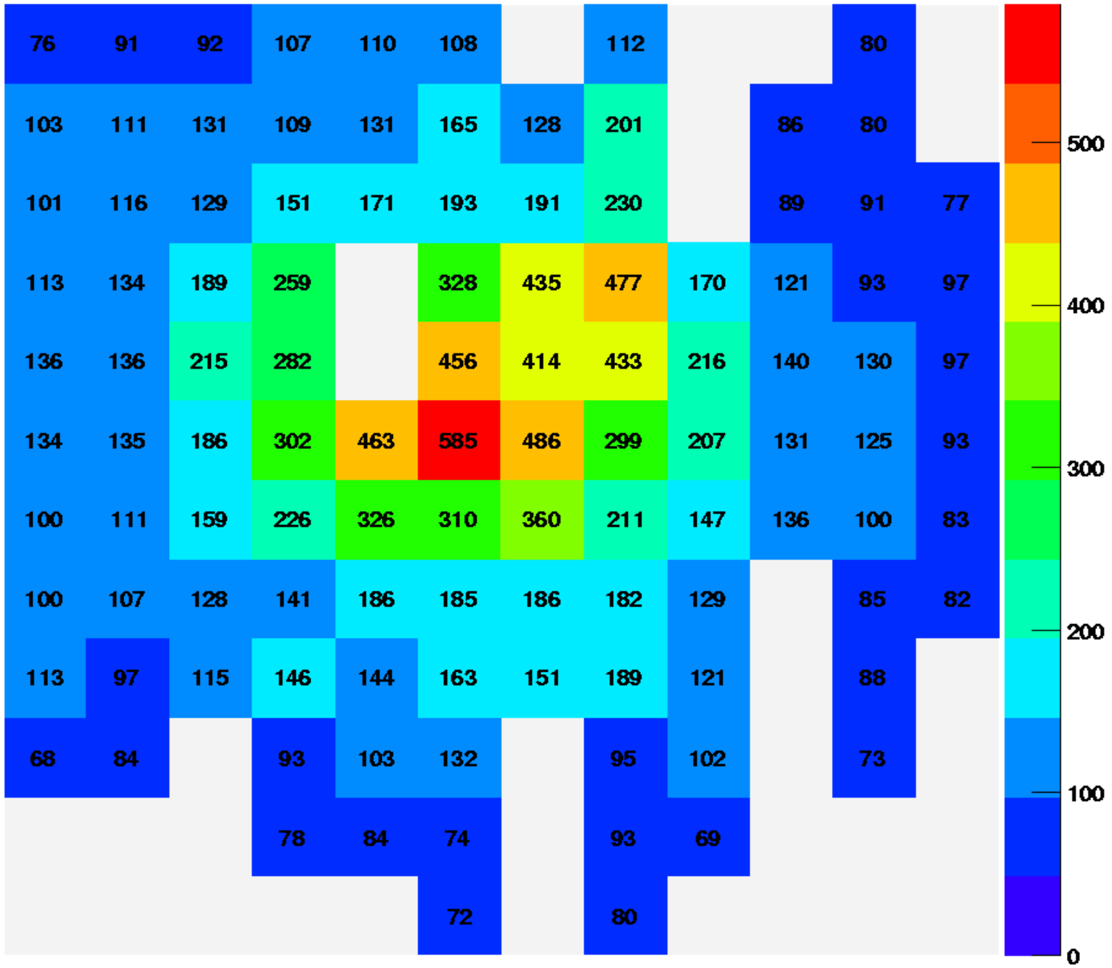

about 10 events/day.

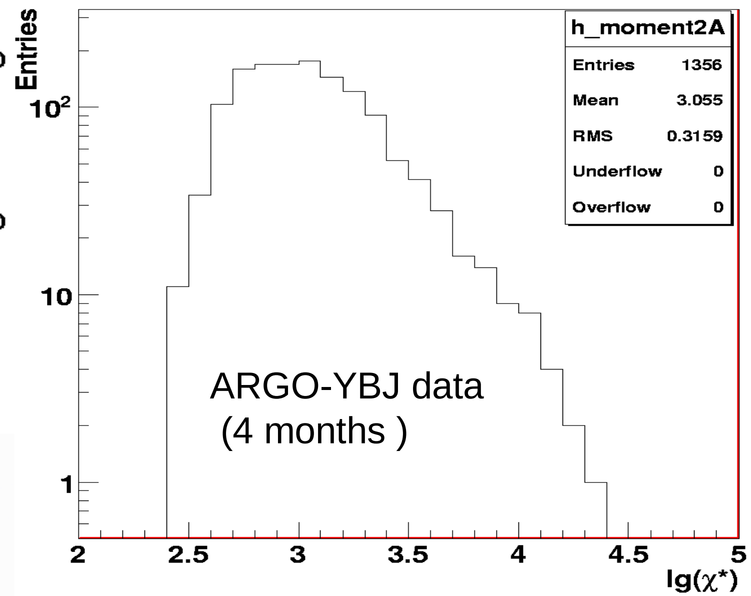

$$\chi = \sqrt{\rho_1 \rho_2 r_{12}}$$

$$\log(\chi) = 2.92$$

ρ(particle/m²), r(m)

J. Zhao, X. Ma -ARGO-YBJ coll. ICRC2011- HE3.1 n.814

Conclusions

1. Antip/p upper limits have been set @ TeV energies

2. IMF has been measured (and the capability of the method for forecasting solar magnetic storms has been demonstrated).

3. Anisotropy has been measured both at large and medium scale

4. pp cross section has been measured up to 100 TeV in the lab frame.

5. light component of CR (p+He) has been measured below 100 TeV.

- The analog readout extends the energy range up to PeV.

- The core region is measured with unprecedented detail.

- Many physics items have been made accessible, namely p-p cross section at PeV energies , primary mass identification and composition around the knee, test of interaction models and shower core study .